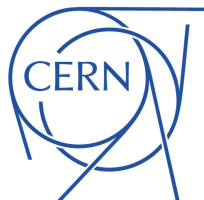




Recent Searches for *New Resonances*
and *Contact Interactions* with **ATLAS**

CERN LHC Seminar

April 25th, 2017



Arely Cortes-Gonzalez

(CERN)

On behalf of the **ATLAS Collaboration**



Recent Searches for *New Resonances*
and *Contact Interactions* with **ATLAS**

CERN LHC Seminar

April 25th, 2017

*2015 and 2016
dataset!*



Arely Cortes-Gonzalez

(CERN)

On behalf of the **ATLAS Collaboration**

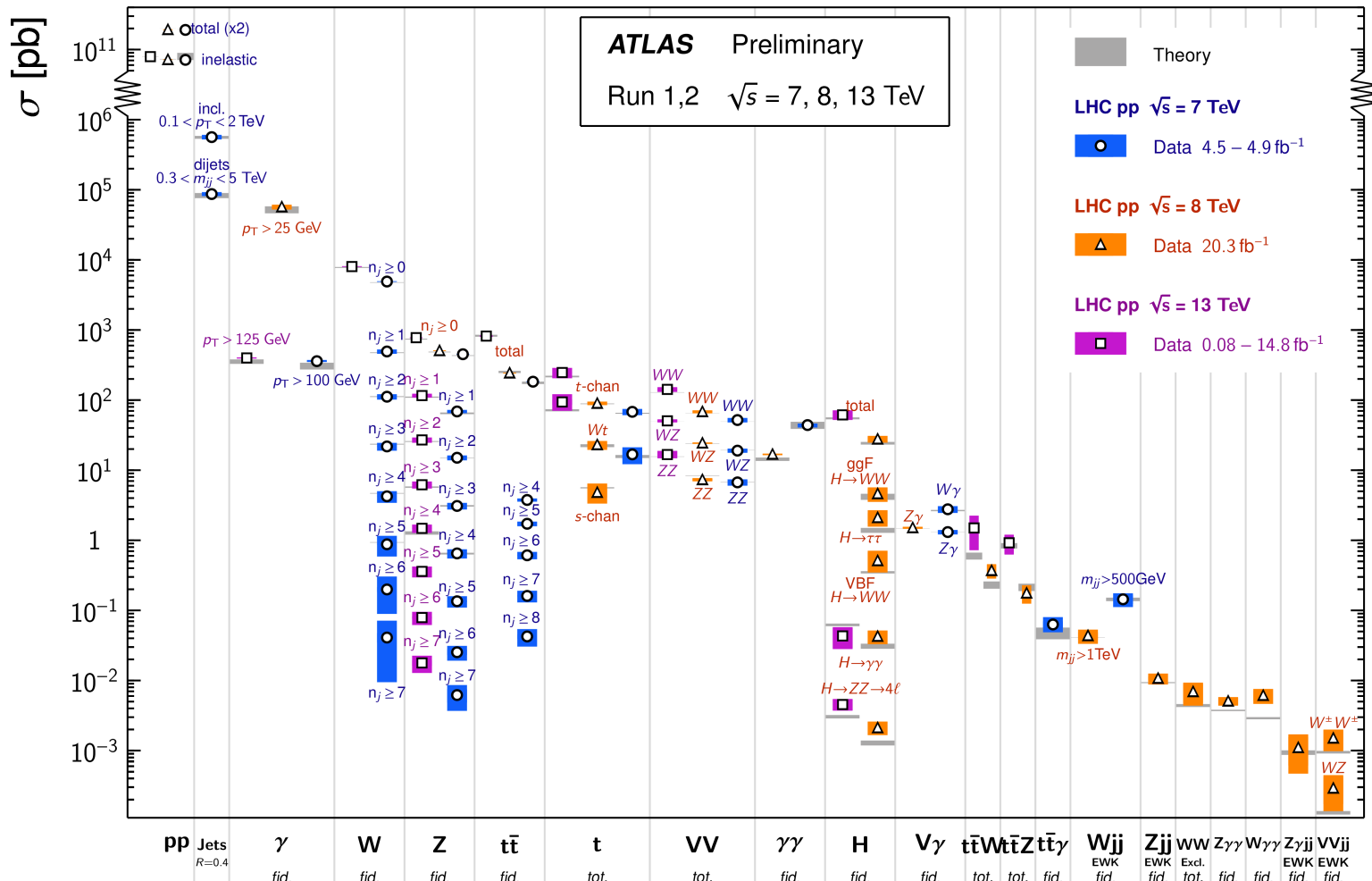
Standard Model

Very **successful** theory.

* **Precise measurements** in great agreement with predictions.

Standard Model Production Cross Section Measurements

Status: March 2017



Standard Model

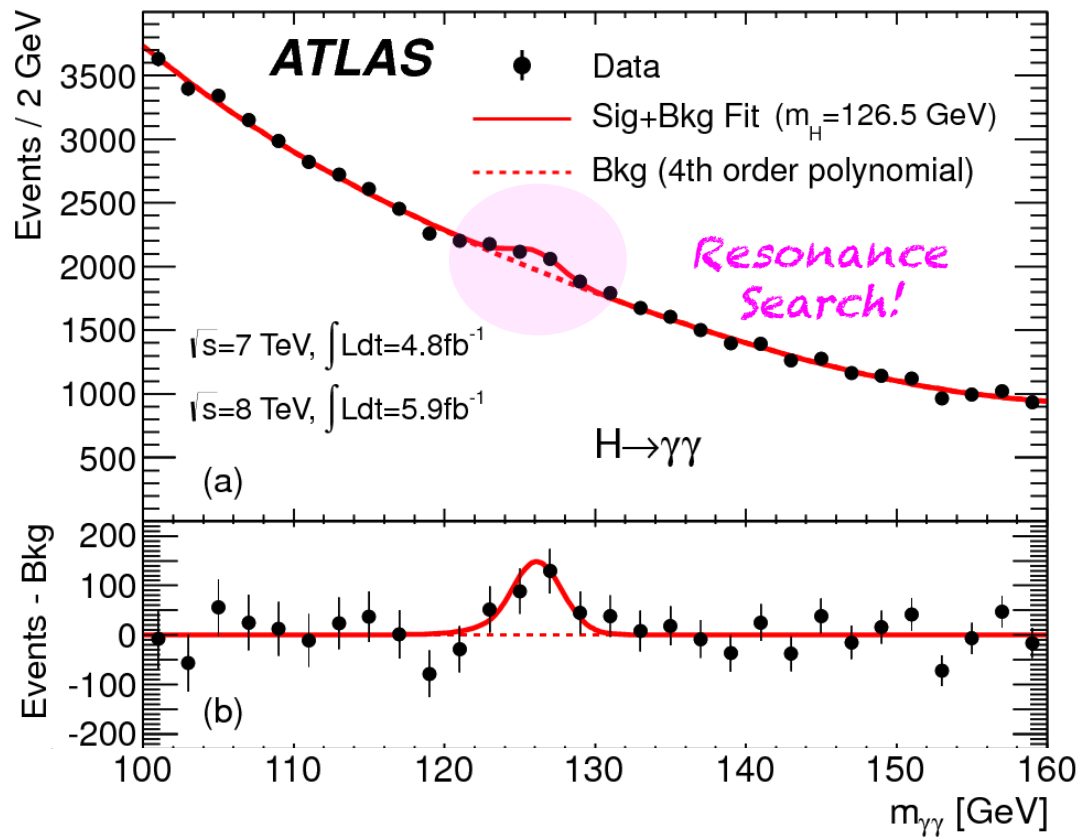
Phys. Lett. B 716 (2012) 1-29

The **Higgs discovery** further validated the SM
(*self-consistent theory*).

Run I *legacy*: Higgs discovery
The discovery of a new particle
also opened a new channel for
searches.

Still left with many open
questions....

e.g. High-levels of **fine tuning**
needed to avoid divergences in
Higgs mass corrections.



Why **BSM**?

SM is a self-consistent theory, with predictions in agreement with measurements, but...

- * **Hierarchy** problem (of mass scales).

Large discrepancy between weak force and gravity: $m_{EW}/m_{Planck} \sim 10^{-16}$.

- * **Fine tuning** needed to avoid divergences in Higgs mass corrections.

- * No **Dark matter** candidate.

- * Baryon **asymmetry**.

- * **Neutrino** masses.

Why **BSM**?

SM is a self-consistent theory, with predictions in agreement with measurements, but...

* **Hierarchy** problem (of mass scales).

Large discrepancy between weak force and gravity: $m_{EW}/m_{Planck} \sim 10^{-16}$.

* **Fine tuning** needed to avoid divergences in Higgs mass corrections.

* No **Dark matter** candidate.

* Baryon **asymmetry**.

* **Neutrino** masses.

How to solve these?

* **SUSY.**

* **Extra Dimensions.**

* **Compositeness.**

* **Sequential Standard Model.**

* **Hidden Sectors.**

* **Top partners,**

* **... New TeV scale interactions/
particles!**

Why **BSM**?

SM is a self-consistent theory, with predictions in agreement with measurements, but...

- * **Hierarchy** problem (of mass scales).

Large discrepancy between weak force and gravity: $m_{EW}/m_{Planck} \sim 10^{-16}$.

- * **Fine tuning** needed to avoid divergences in Higgs mass corrections.

- * No **Dark matter** candidate.

- * Baryon **asymmetry**.

- * **Neutrino** masses.

- * **Excited** states of leptons and quarks (q^*) can be predicted from **composite models**.

Explains generational structure and mass hierarchy of quarks.

- * **Composite Higgs**

Heavy Vector triplet model (**HVT**), with new W'^{\pm} , Z' states.

- Model A: *Extended gauge symmetry*.
- Model B: *Minimal composite Higgs model*.

Why **BSM**?

SM is a self-consistent theory, with predictions in agreement with measurements, but...

- * **Hierarchy** problem (of mass scales).

Large discrepancy between weak force and gravity: $m_{EW}/m_{Planck} \sim 10^{-16}$.

- * **Fine tuning** needed to avoid divergences in Higgs mass corrections.

- * No **Dark matter** candidate.

- * Baryon **asymmetry**.

- * **Neutrino** masses.

Several extensions of the SM with extended gauge symmetries.

- * **Sequential Standard Model.**

SM + new spin-1 heavy gauge bosons with similar couplings as SM W^\pm and Z.

New bosons at the TeV scale.

Why **BSM**?

SM is a self-consistent theory, with predictions in agreement with measurements, but...

- * **Hierarchy** problem (of mass scales).

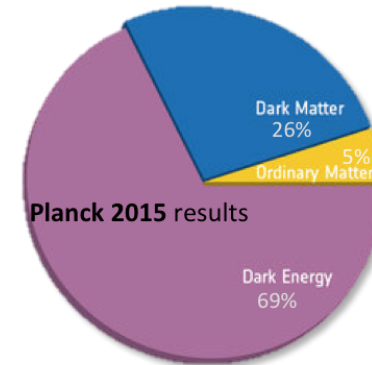
Large discrepancy between weak force and gravity: $m_{EW}/m_{Planck} \sim 10^{-16}$.

- * **Fine tuning** needed to avoid divergences in Higgs mass corrections.

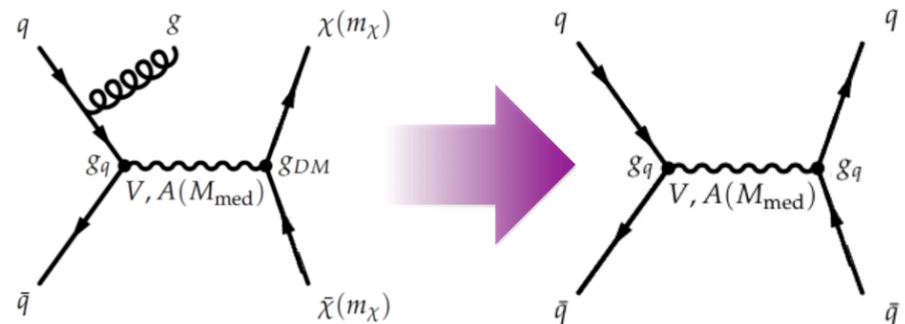
- * No **Dark matter** candidate.

- * Baryon **asymmetry**.

- * **Neutrino** masses.

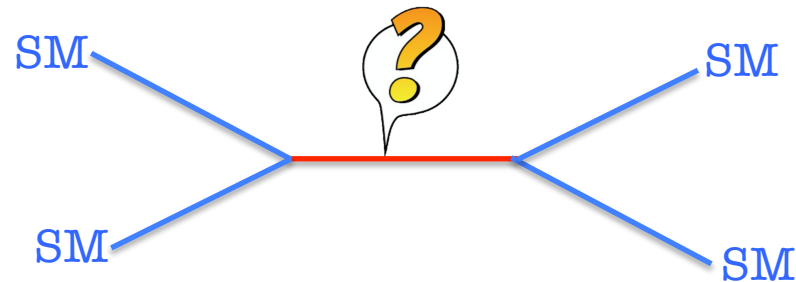
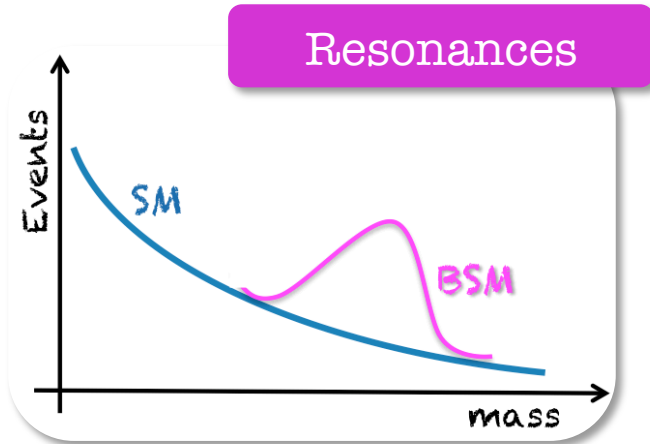


*Resonance searches can also be interpreted in terms of **DM models**.*



Searching...

We look for observations of new resonances in the ***tails of the SM distributions***.
 These resonances could decay into e.g. vector bosons or fermions.



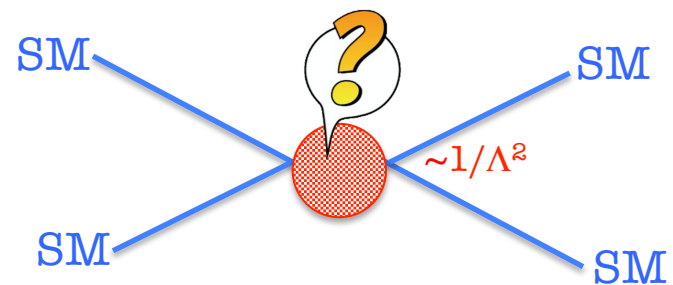
SM background can be modeled in a data driven fashion.

Different searches sensitive to **narrow** resonances (*wide variety of **signatures** to be explored!*).

- * Fully hadronic
 - di-jet, $V(qq)+H(qq)$
- * With leptons
 - dileptons, lepton + E_T^{miss}
- * with Photons
 - photon + E_T^{miss}

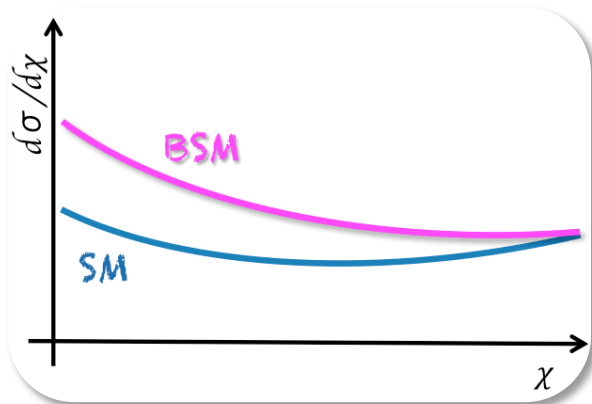
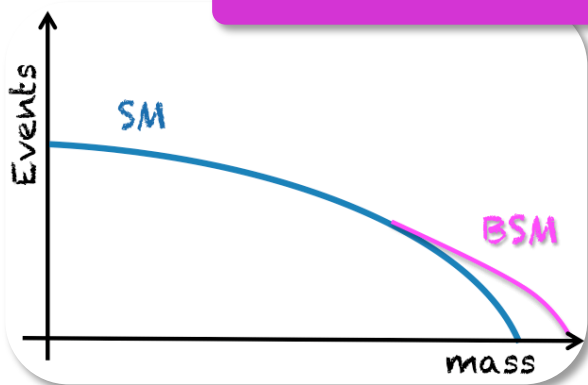
Searching...

We look for modifications in angular and mass distributions arising from **new contact interaction (CI) scales**.



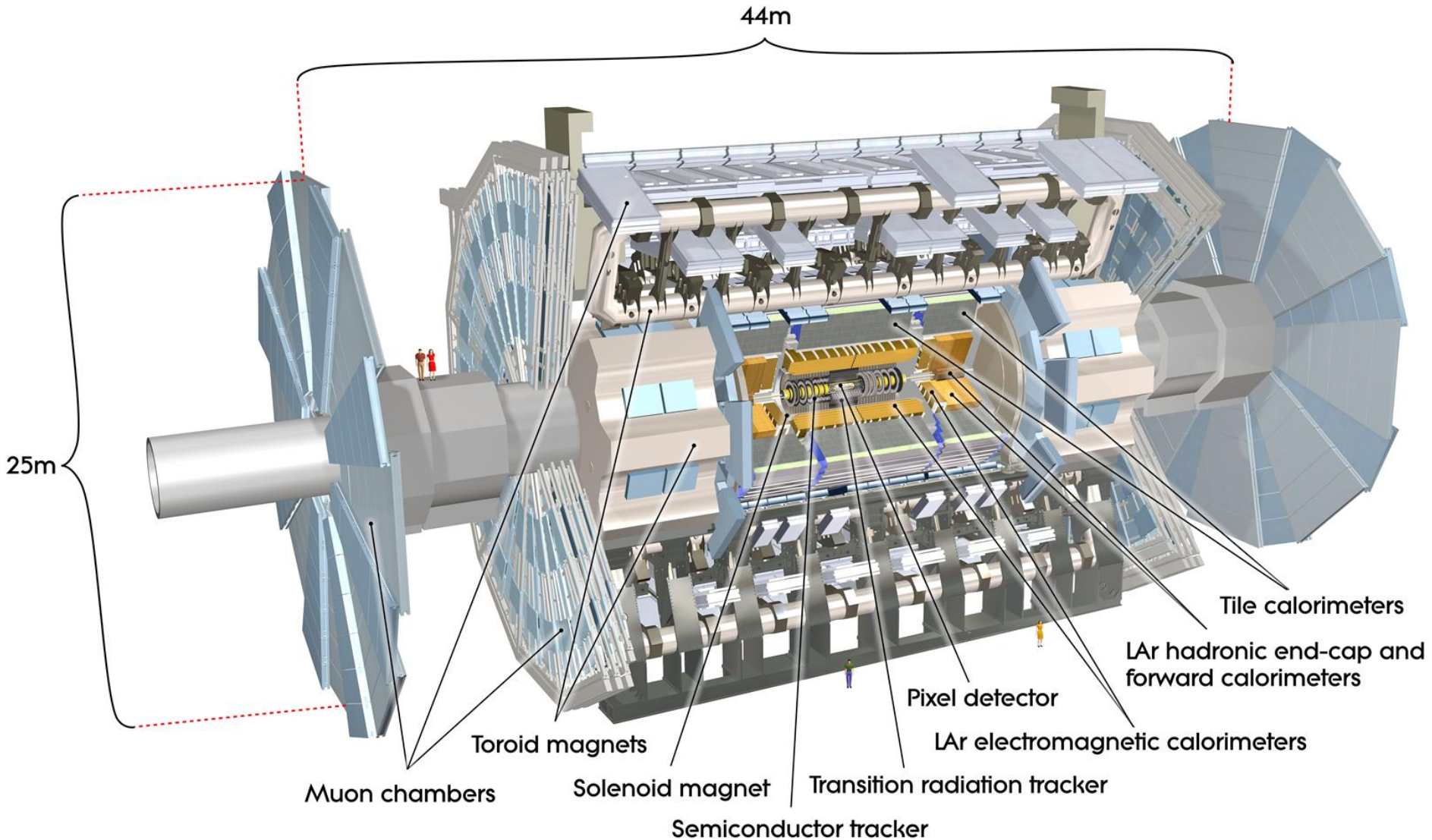
New **mediating particle** with a mass much higher than the energy exchange modeled as contact interaction with new physics at **energy scale Λ** .

Contact Interactions



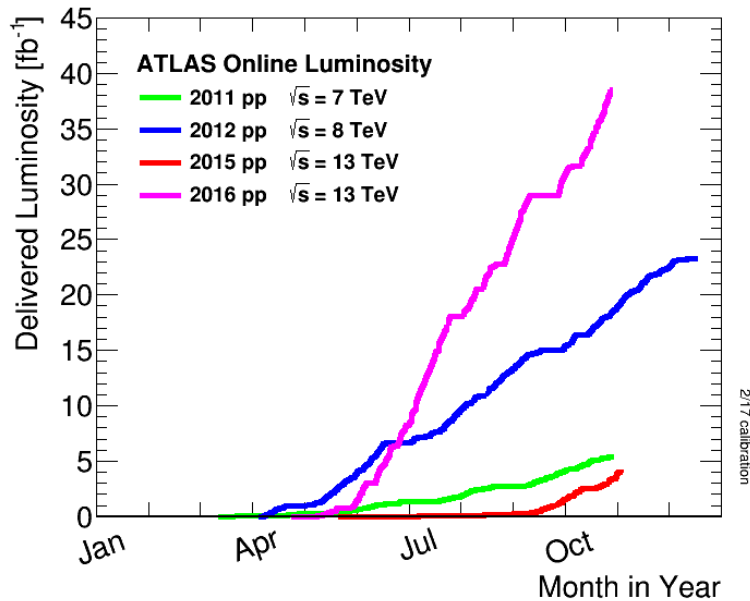
- * Dileptons
 - Broad excess in invariant mass distributions.
- * Dijets
 - CI is often more isotropic than QCD → use angular information.

ATLAS Detector

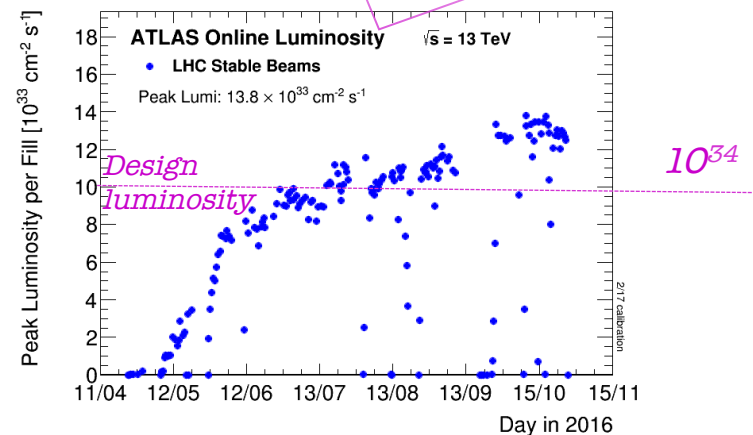
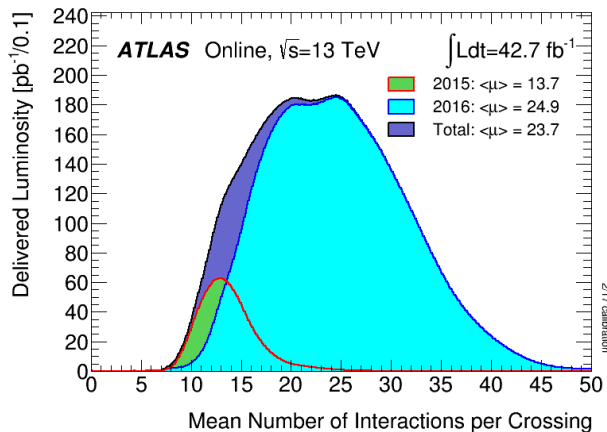
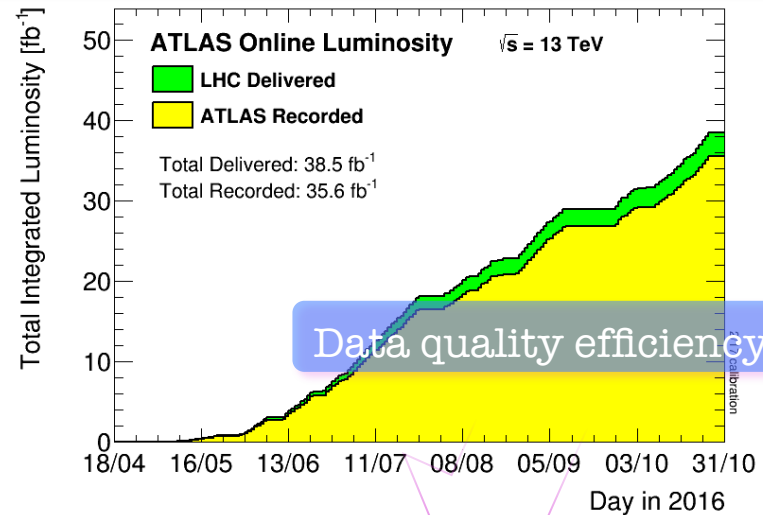


ATLAS Data

Excellent **performance by the LHC** and high **data taking efficiency** by detectors in the **13 TeV pp** collisions period (2015, 2016).

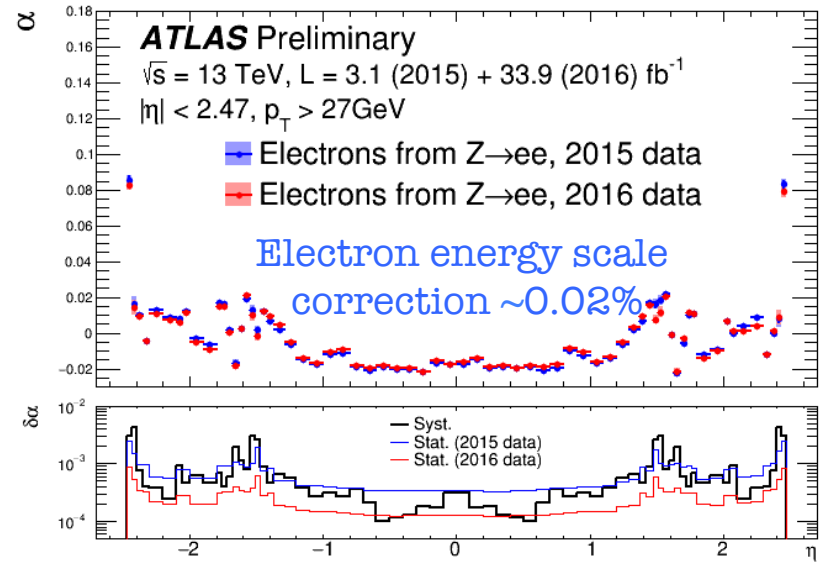
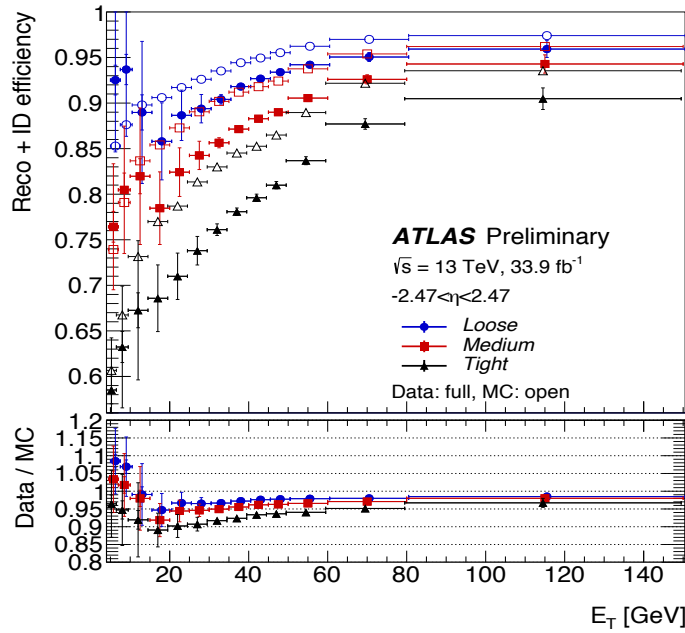


$\sim 40 \text{ fb}^{-1}$ @ 13 TeV recorded in 2015 and 2016

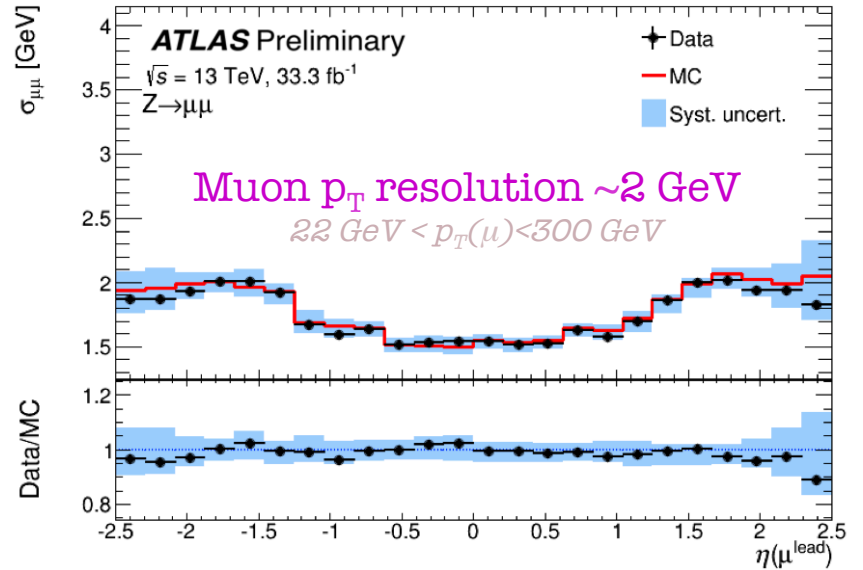
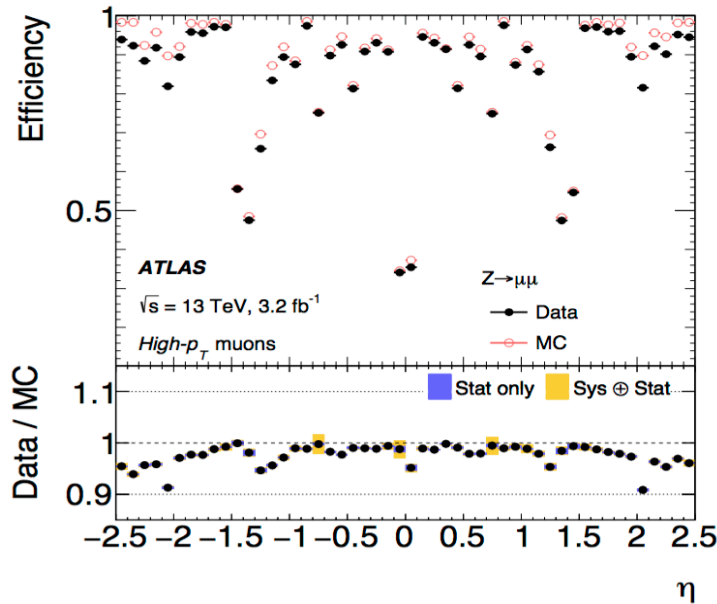


Performance: Leptons

Electrons

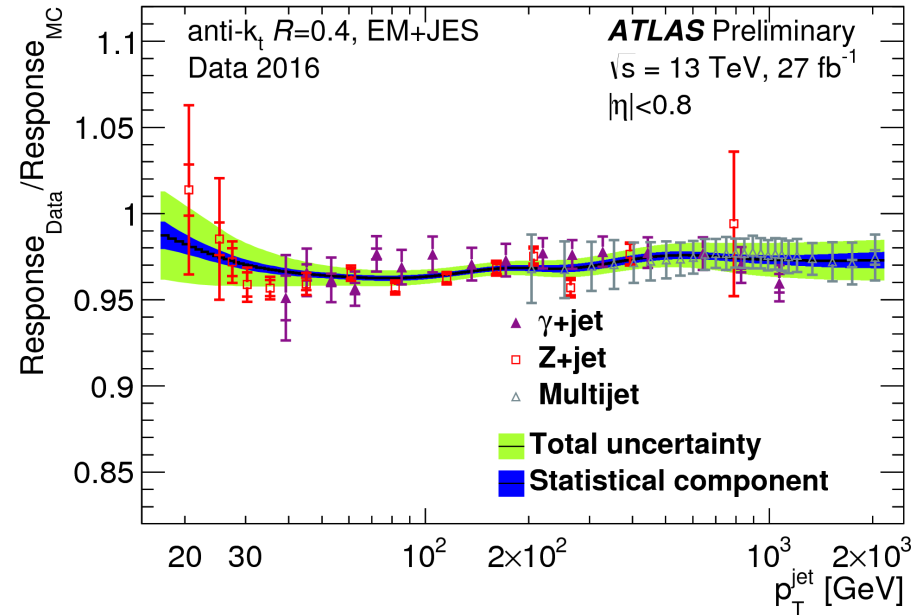
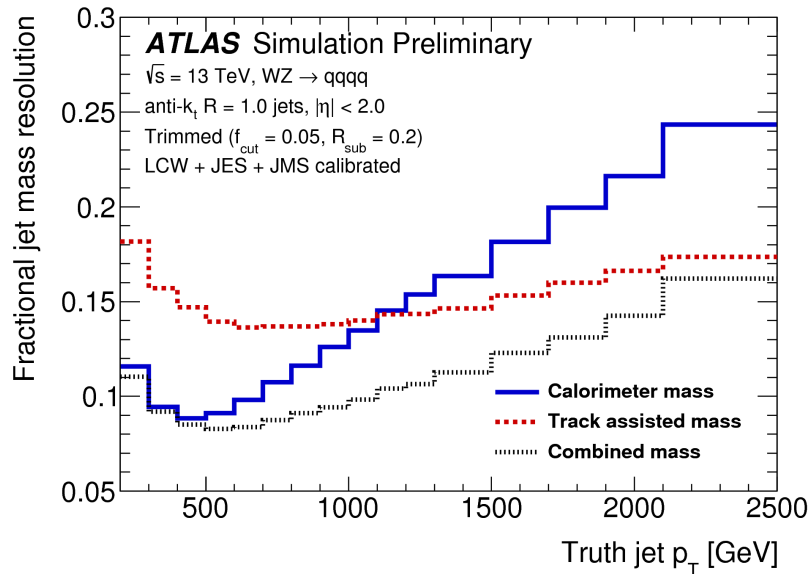


Muons



Jets

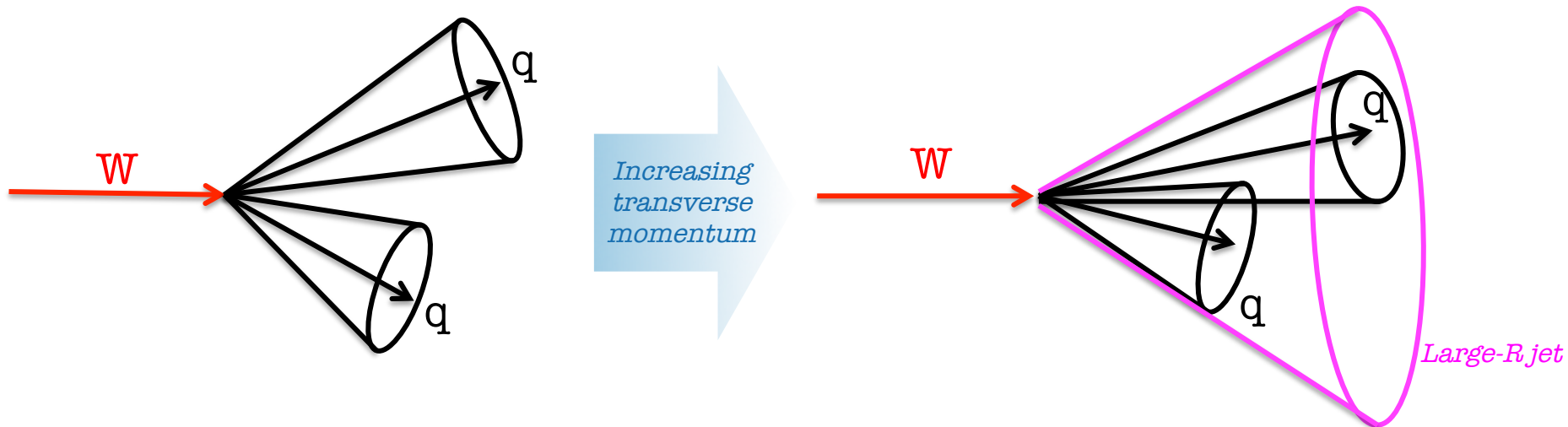
Analyses rely on a good understanding of **jet calibration** up to multi-TeV scale.



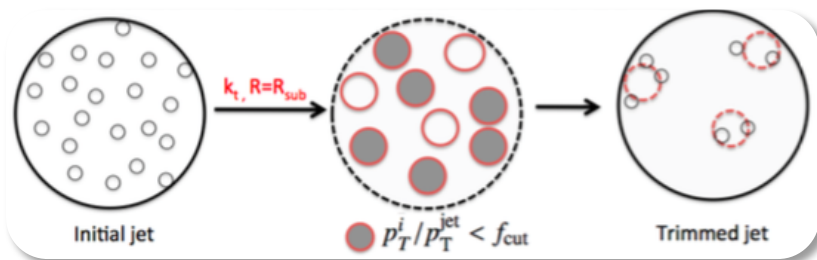
Jet mass improvements

Optimizes **large-R jet mass** computed using combination of calorimeter and tracking information

$$m_J \equiv w_{\text{calo}} \times m_J^{\text{calo}} + w_{\text{track}} \times \left(m_J^{\text{track}} \frac{p_T^{\text{calo}}}{p_T^{\text{track}}} \right)$$



Energy depositions in calorimeter used to form topological clusters:
reconstruct **large R-jets: Anti- k_r , $R=1.0$ jets.**



Re-cluster with $R_{\text{sub}} = 0.2$.
Remove sub-jets with $f_{\text{cut}} < 0.05$.

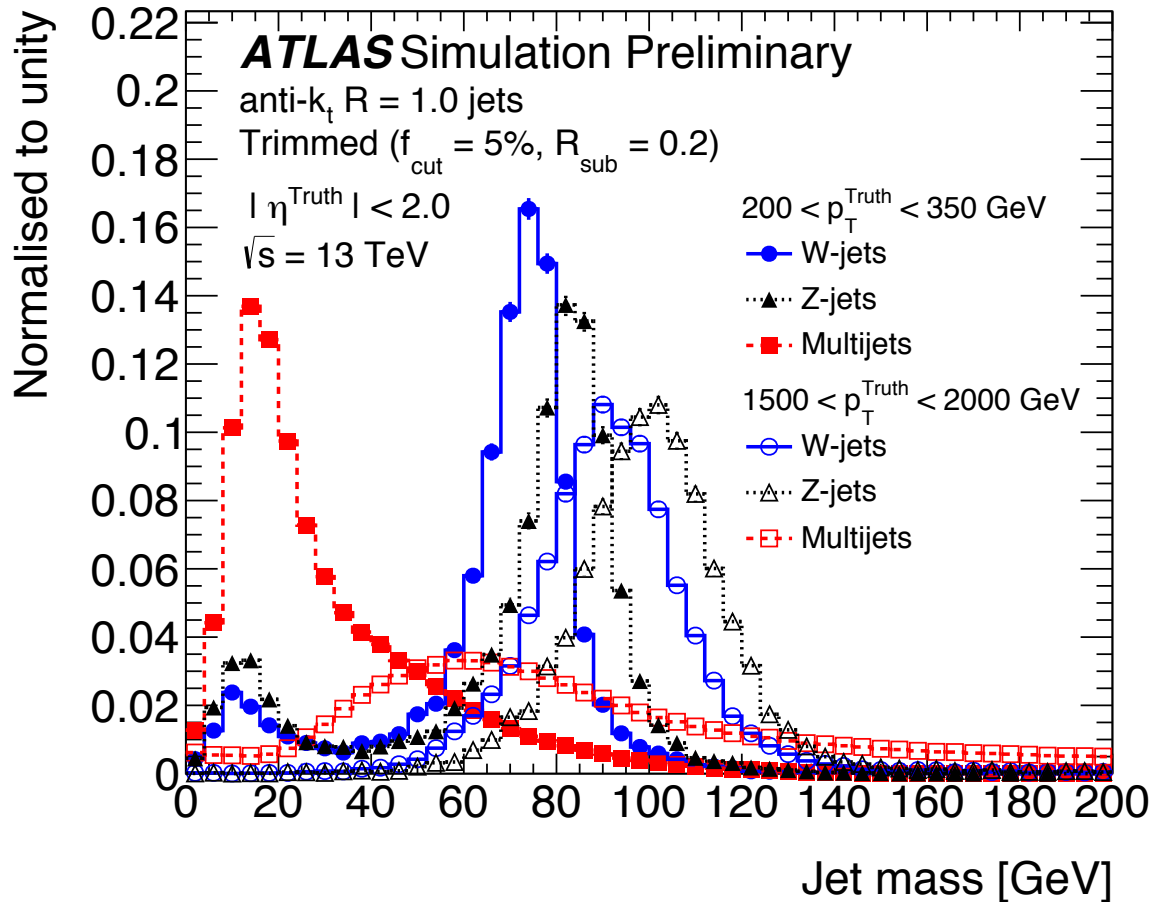
Trimming

Remove softer components
(mainly from UE and pileup).

Improved *mass resolution*.

Discriminating against background: boson tagging.

Use differences in the jet characteristics between signal and background jets.

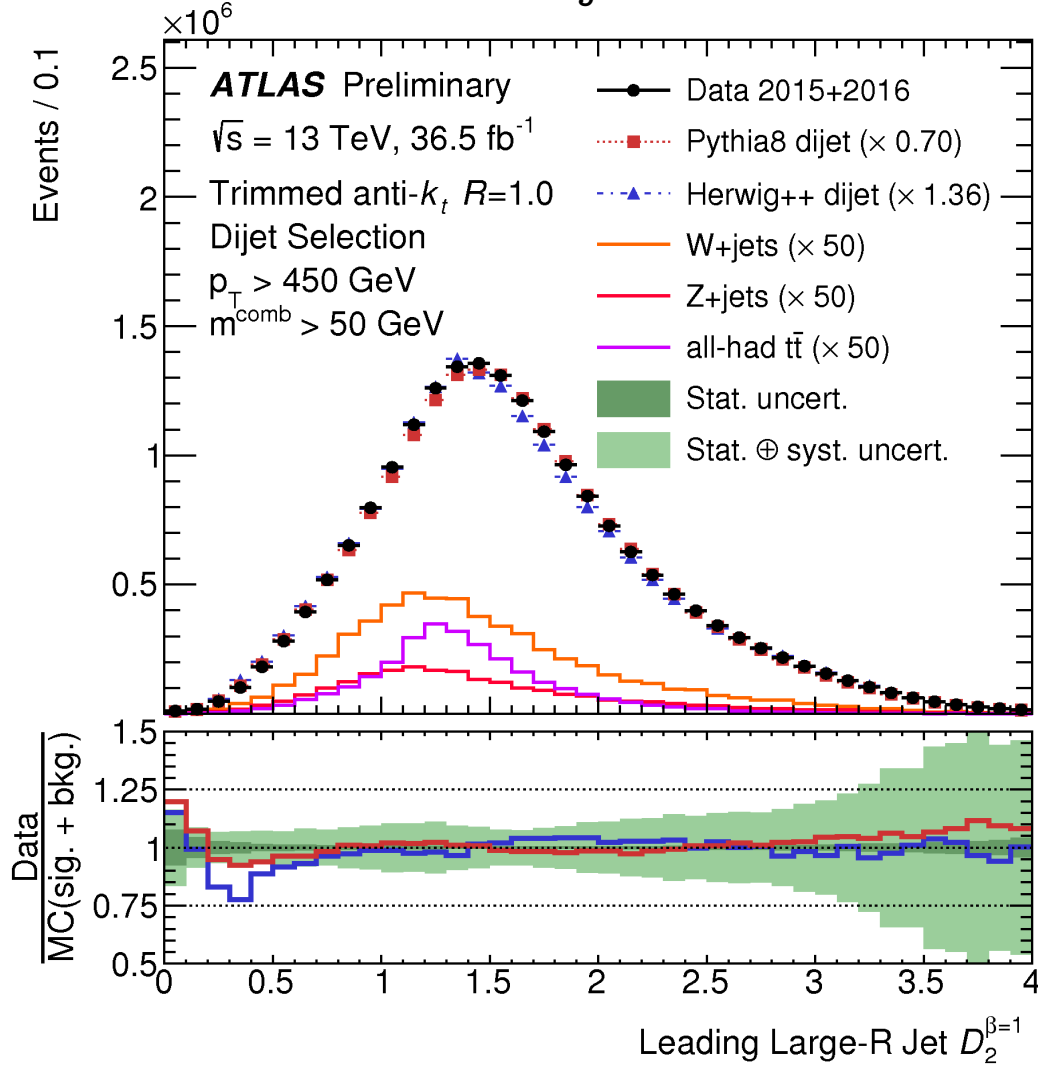


Jet mass is consistent with m_W or m_Z .

Mass windows for W/Z bosons are p_T -dependent.

Discriminating against background: boson tagging.

Use differences in the jet characteristics between signal and background jets.

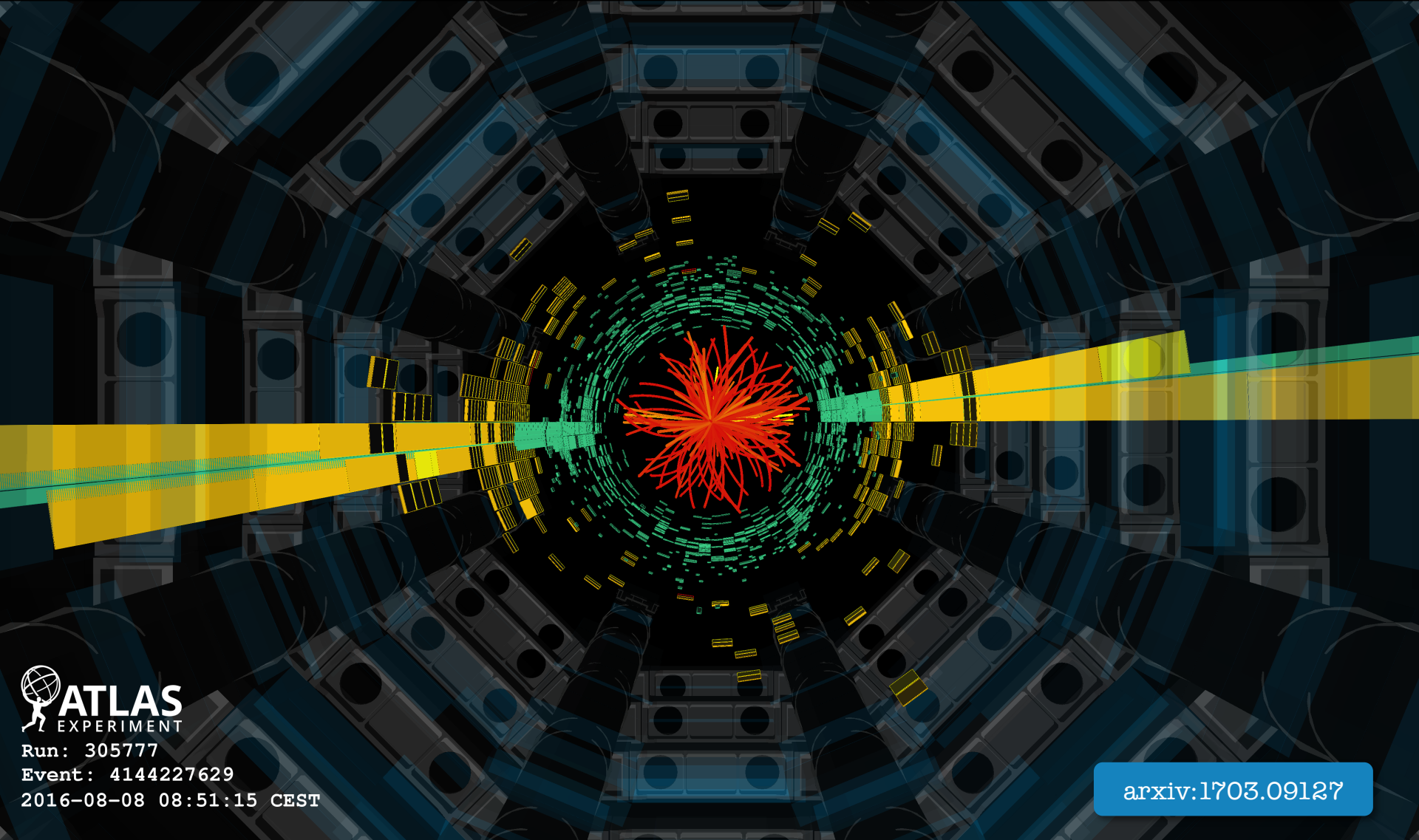


Substructure variable $D_2^{\beta=1}$
 consistent with two prong decays.

$D_2^{\beta=1}$ exploits energy correlations functions to tag boosted objects with two-prong structures.

Constant $\sim 50\%$ efficiency in V -jet p_T for $\sim 2\%$ fake rate.

High Mass **Di-Jet** Search



 **ATLAS**
EXPERIMENT

Run: 305777

Event: 4144227629

2016-08-08 08:51:15 CEST

arxiv:1703.09127

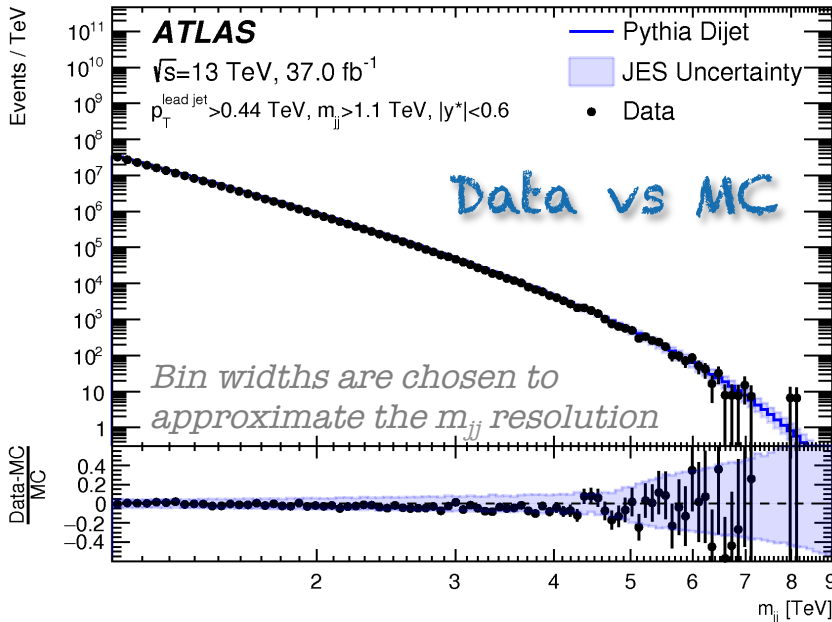
Highest-mass dijet event: $m_{jj} = 8.12 \text{ TeV}$, $|y^| = 0.38$*

Selection

Events selected with lowest un-prescaled single jet trigger ($p_T > 380$ GeV).

	p_T^{leading}	$p_T^{\text{subleading}}$	$ y^* $	$ y_B $	m_{jj}
Resonance	> 0.44 TeV	> 0.06 TeV	< 0.6	-	> 1.1 TeV
W^*	> 0.44 TeV	> 0.06 TeV	< 1.2	-	> 1.7 TeV
Angular	> 0.44 TeV	> 0.06 TeV	< 1.7	< 1.1	> 2.5 TeV

$$|y^*| = |y_1 - y_2|/2 \quad \text{Rejects forward peaking } t\text{-channel QCD processes.}$$



Strategy: **Resonance**

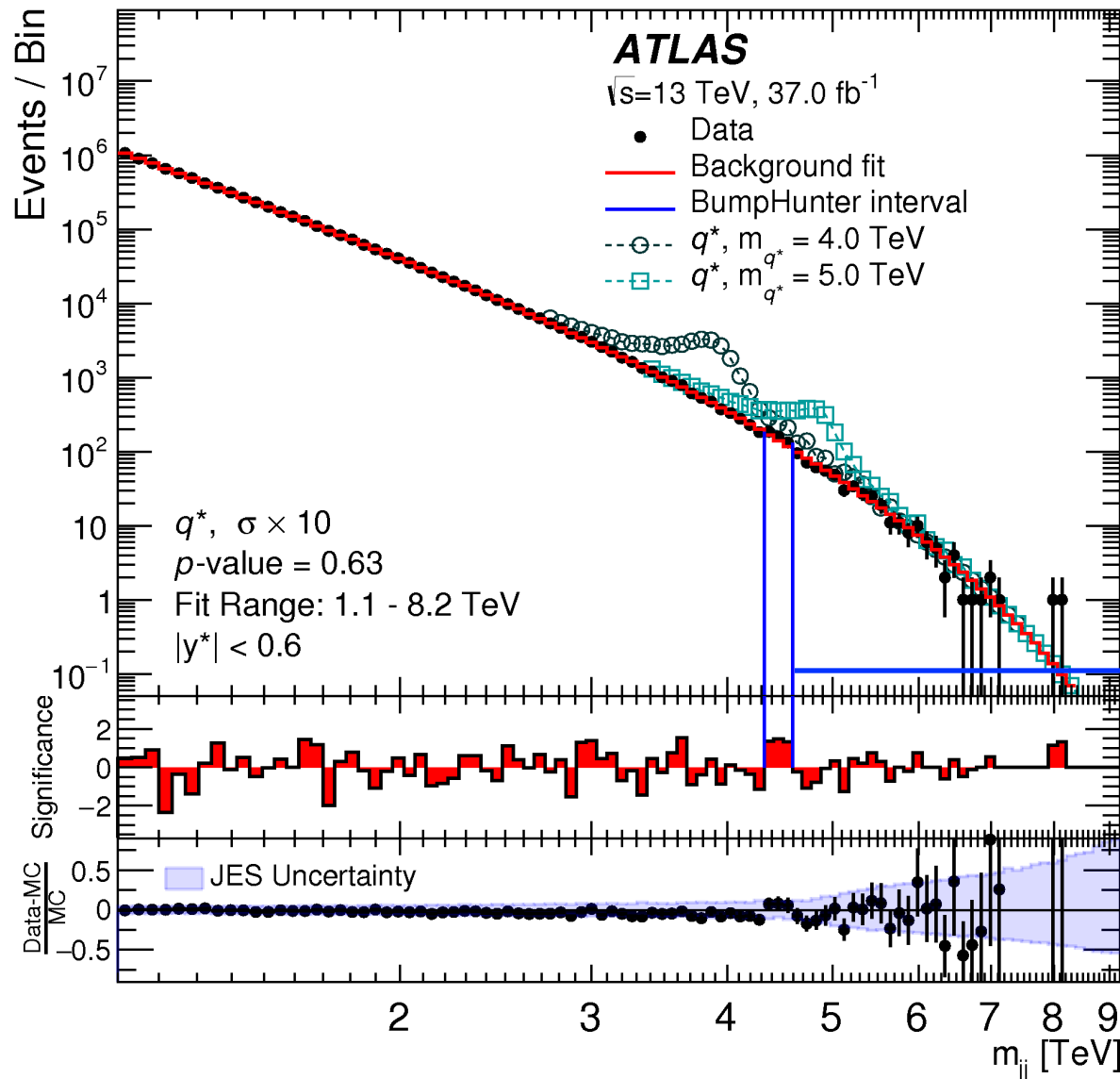
$$f(z) = p_1(1 - z)^{p_2} z^{p_3} z^{p_4} \log z$$

With increasing luminosity and corresponding m_{jj} range extension, a single global fit may not necessarily work.

Sliding Window Fit

NEW

- Perform the $f(z)$ fit in restricted (sliding) ranges (**more flexible!**).
- The limited range allows to use a 3-parameter function.
- Excellent linearity between injected and extracted signal.



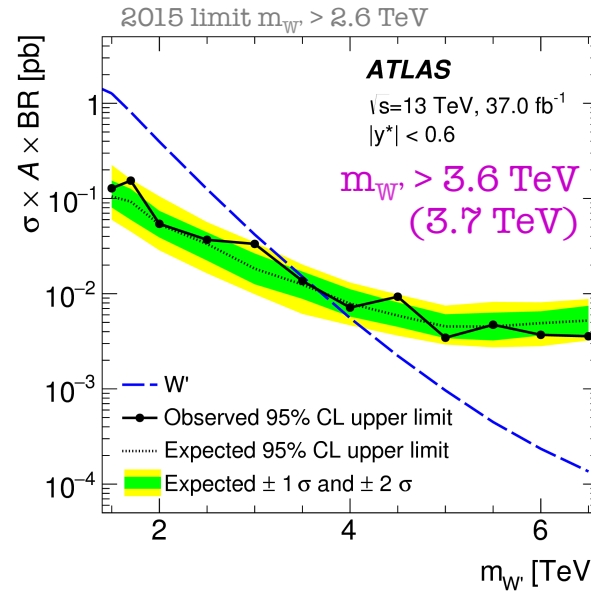
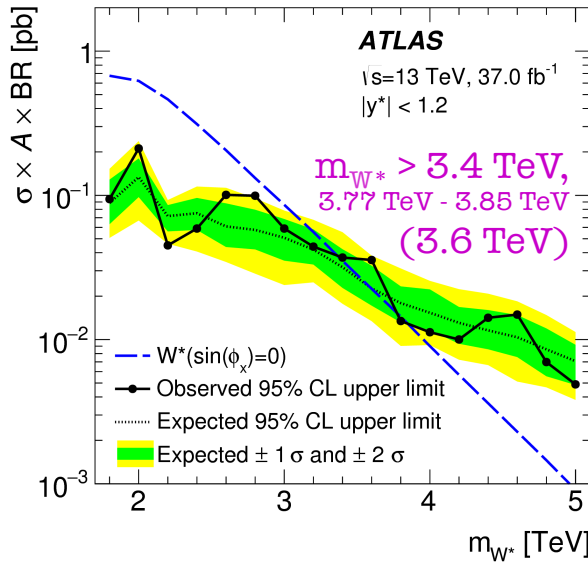
Resonance Search

- **BumpHunter** algorithm compares the binned m_{jj} of data to the fitted bkg estimate.
- Global significance is computed with pseudo-experiments.

Most *discrepant* region:
 (global $p=0.63$) 4326–4595 GeV

No evidence of a localized contribution from **BSM** observed.

High Mass Di-Jet Search

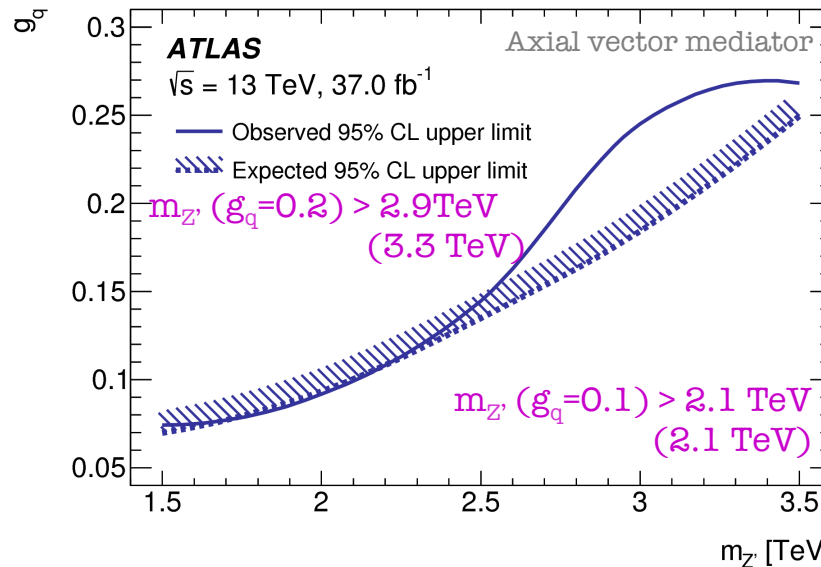
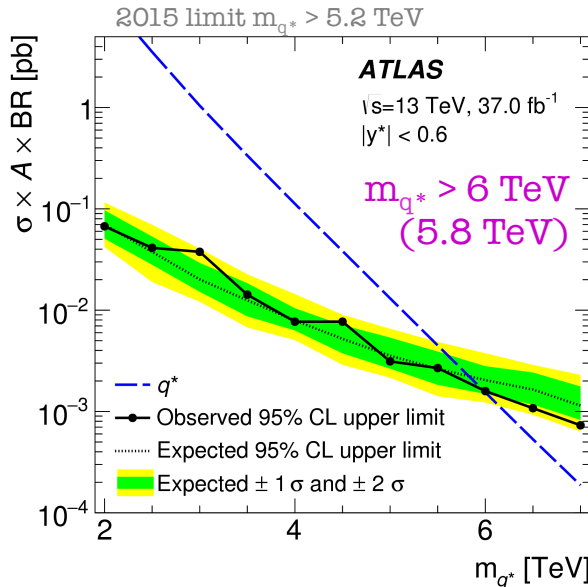


Resonance Limits

95% CL upper observed (expected) limits on the cross section times acceptance for different signal models.

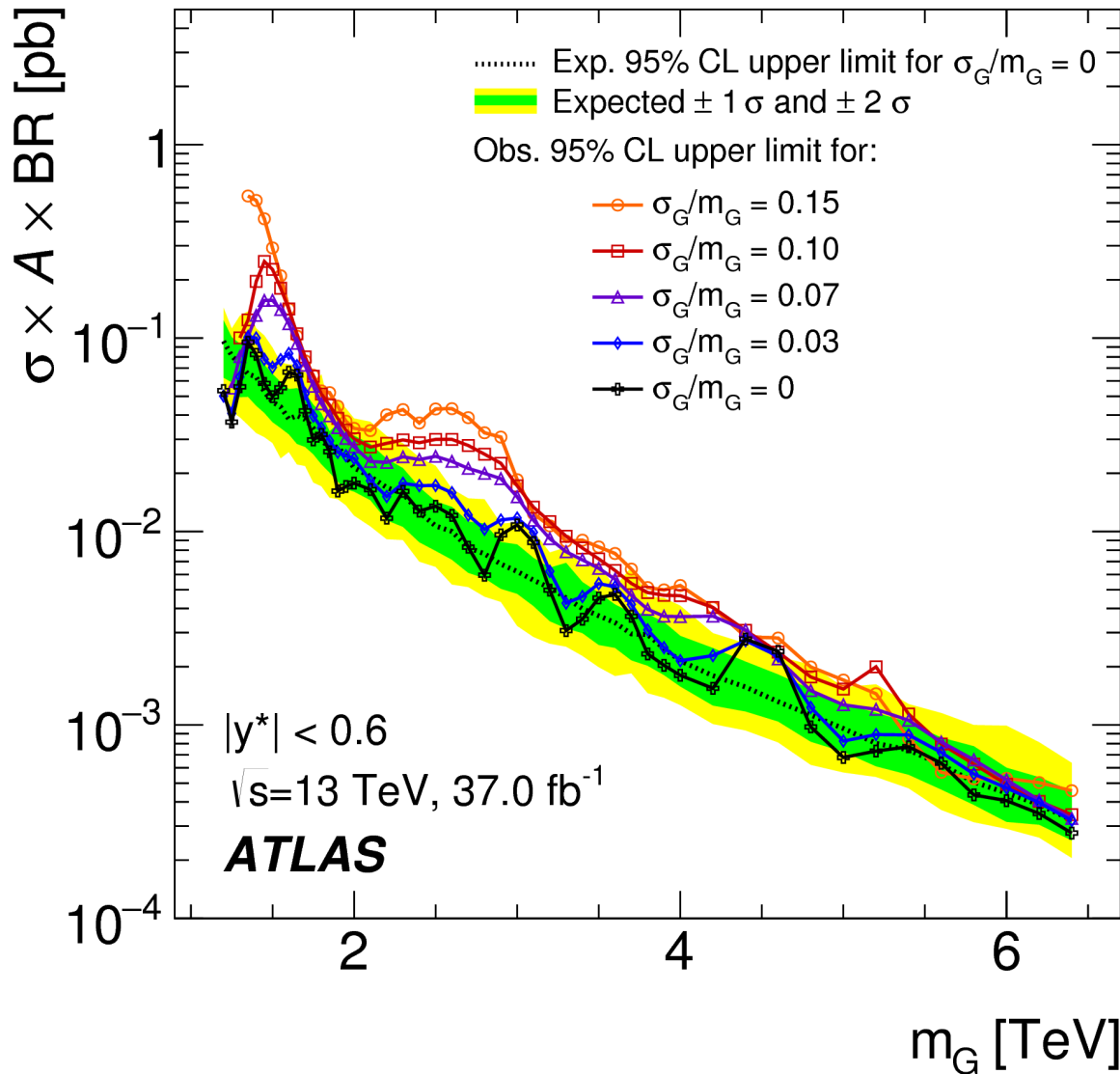
QBH Limits:

$m_{Th} > 8.9$ TeV (8. TeV)



For $g_q=0.6$ the intrinsic width of the Z' in the mass range of interest increases to 15%.

Results limited to $g_q < 0.5$

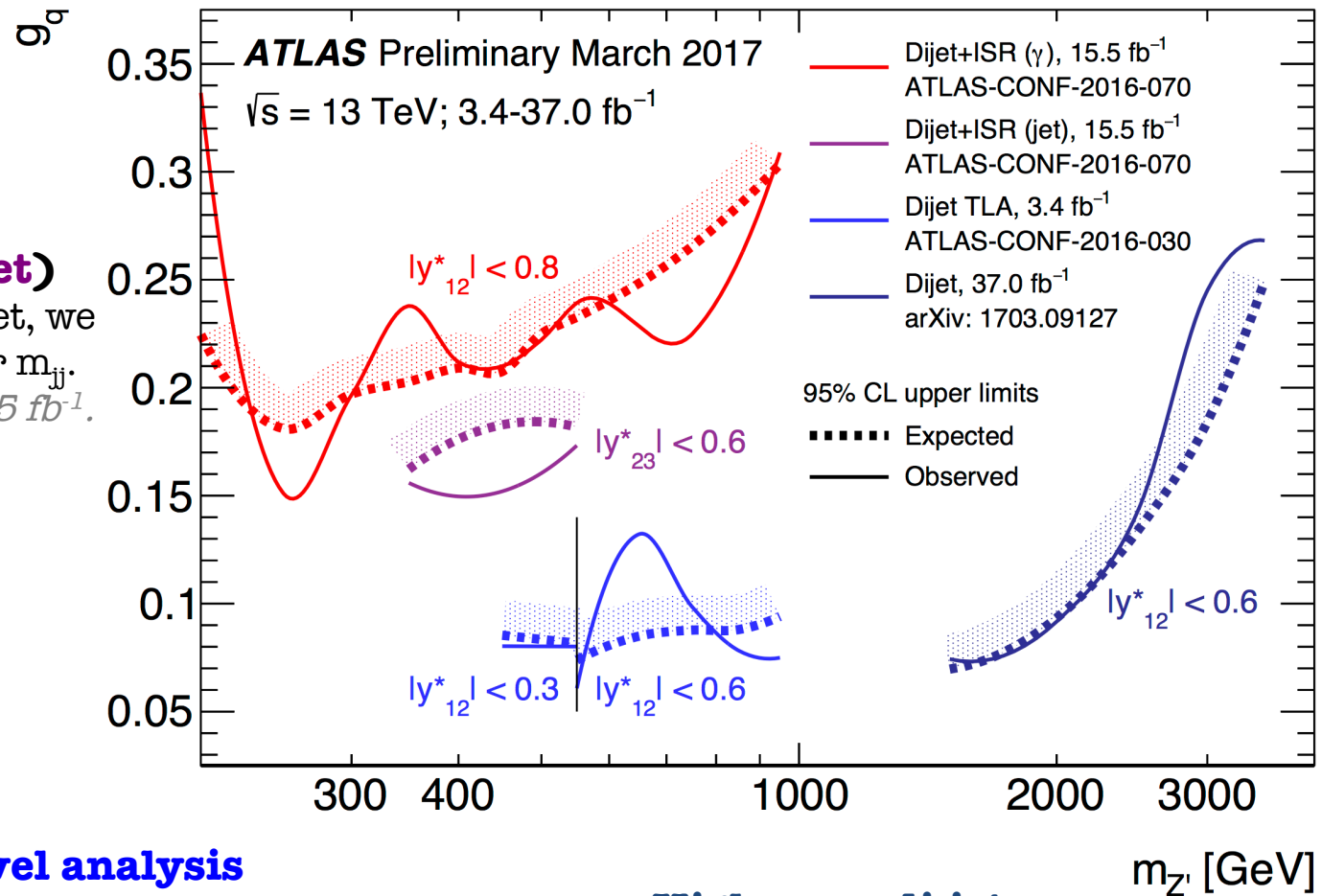


Gaussian Limits

- Limits on *generic Gaussian signals* used to recast results for new signal models.
- Folding method using **NEW** MC based transfer matrix used to factorized out physics and detector effects.
 - The predicted signals can now be compared at *particle level* (assuming Gaussian signal shape).

Di-Jet searches covering the low and high mass regime!

Di-jet + ISR (γ /jet)
 Triggering on ISR γ /jet, we
 can also reach lower m_{jj} .
Last results with 15.5 fb⁻¹.

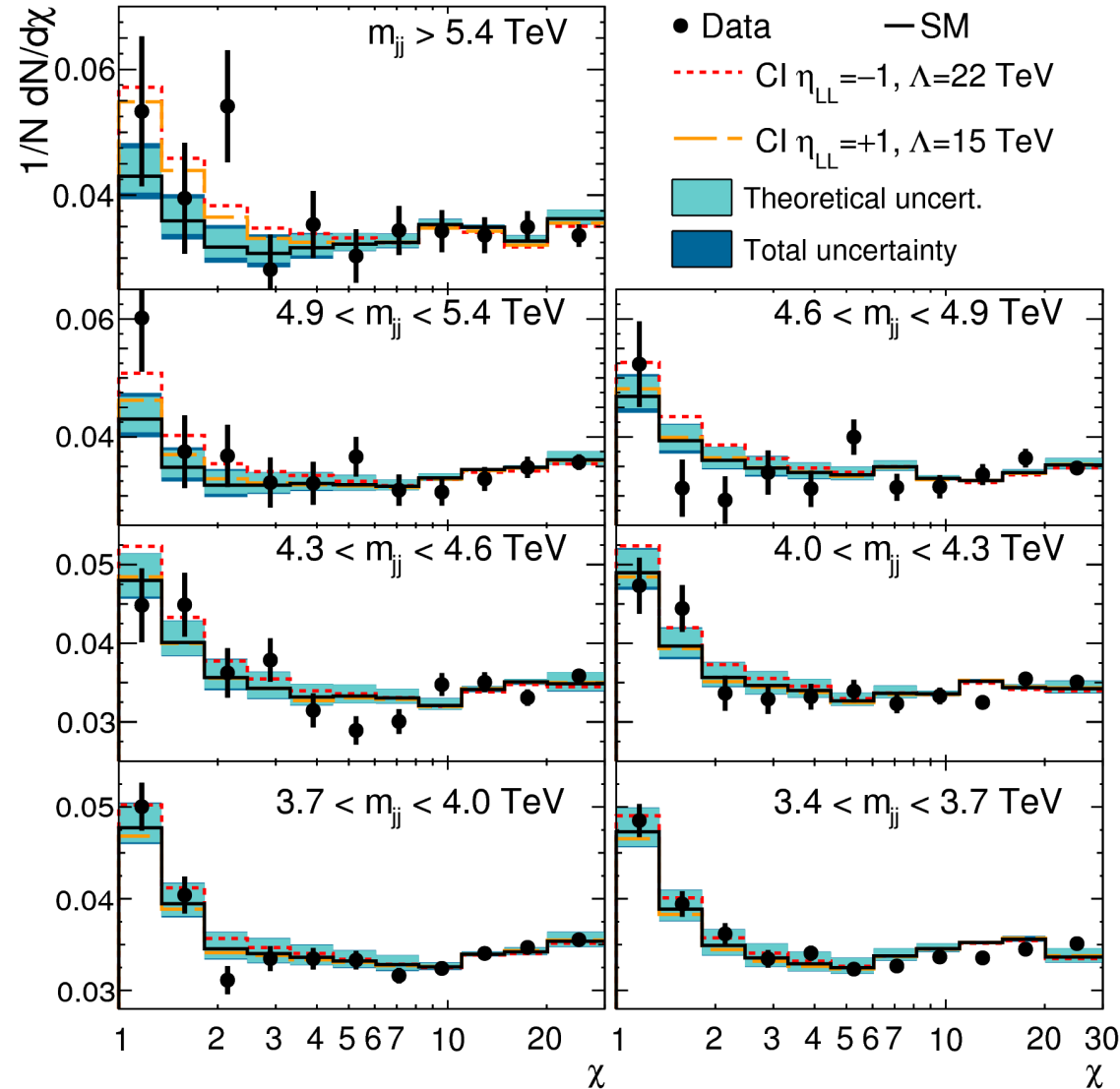


Trigger level analysis

*Strategy: reduce data size/complexity
 to increase rate of recorded data.
 Last results with 3.4 fb⁻¹.*

High mass di-jets

*Reach at low masses limited by
 trigger bandwidth and storage.*

$\sqrt{s}=13$ TeV, 37.0 fb $^{-1}$ **ATLAS**Strategy: **Angular**

$$\chi = e^{2|y^*|} \sim \frac{1 + \cos \theta^*}{1 - \cos \theta^*}$$

Background prediction based on Pythia (used as template) corrected for **NLO** and **EW** effects.

○ Correction factors are mass and angle dependent.

Uncertainties:

○ Jet Energy Scale is the dominant experimental uncertainty.

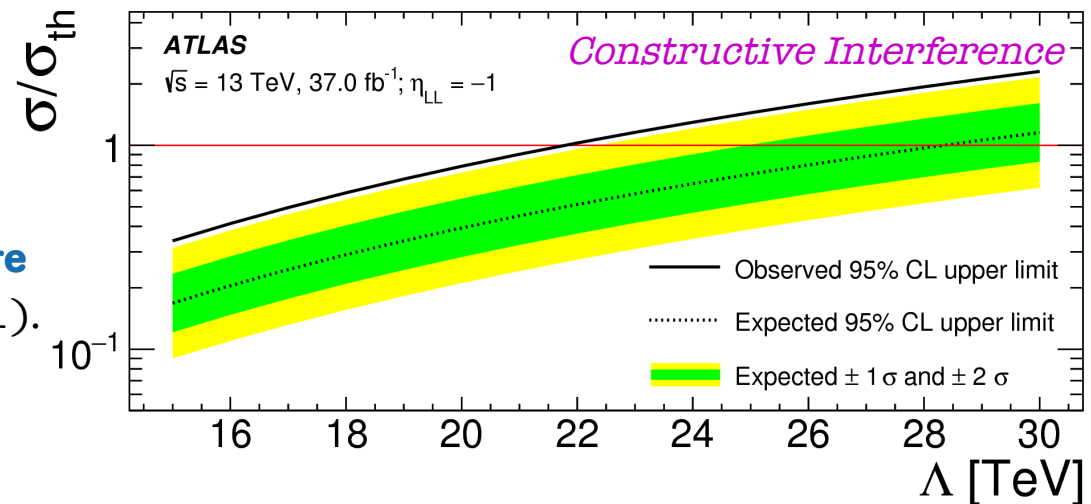
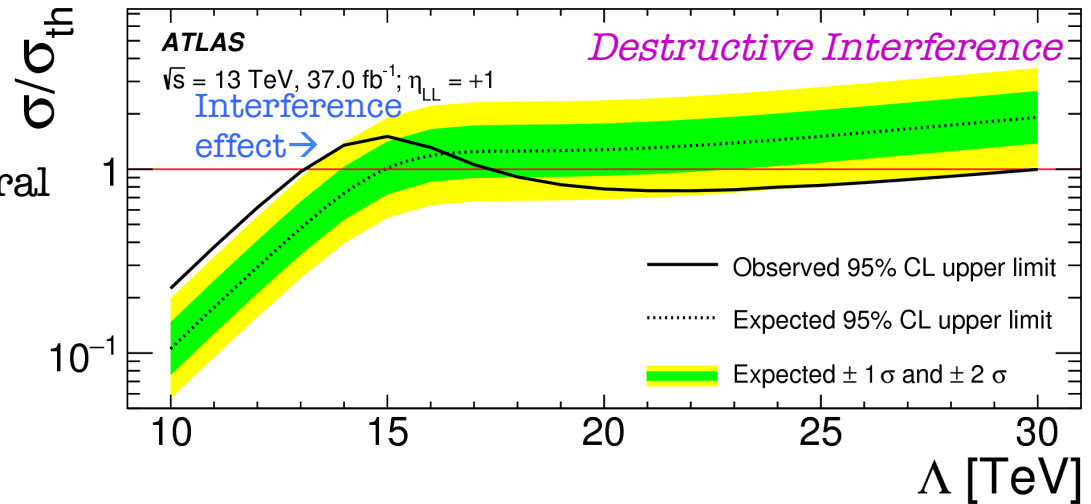
○ Main theoretical uncertainties: renormalization and factorization scales, PDFs.

Angular Limits

- Limits on CI with non-zero left-chiral color coupling.
- Resulting angular distribution is representative of other BSM models (e.g. Z').

$$\mathcal{L}_{qq} = \frac{2\pi}{\Lambda^2} [\eta_{LL} (\bar{q}_L \gamma^\mu q_L) (\bar{q}_L \gamma_\mu q_L) + \cancel{\eta_{RR}} (\bar{q}_R \gamma^\mu q_R) (\bar{q}_R \gamma_\mu q_R) + 2\cancel{\eta_{RL}} (\bar{q}_R \gamma^\mu q_R) (\bar{q}_L \gamma_\mu q_L)]$$

- Both **destructive** and **constructive** interference are considered ($\eta_{LL} = \pm 1$).

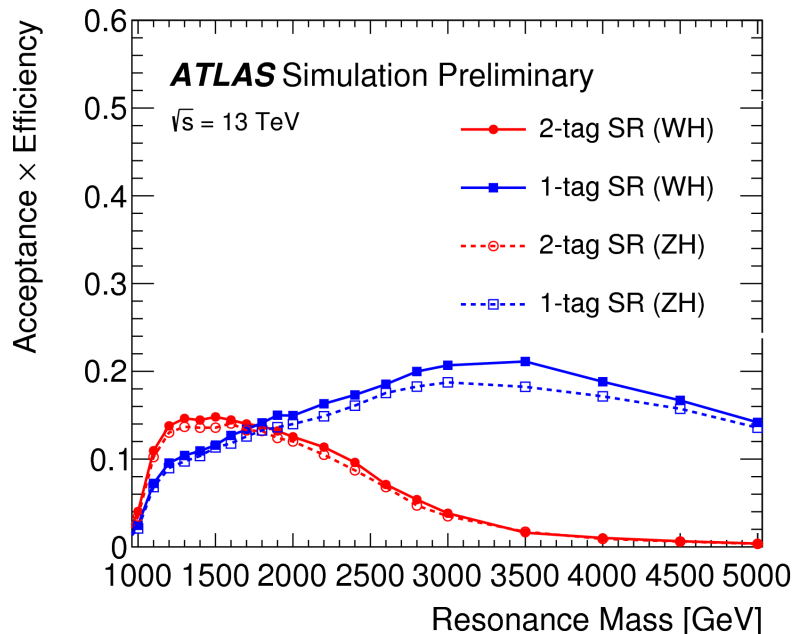
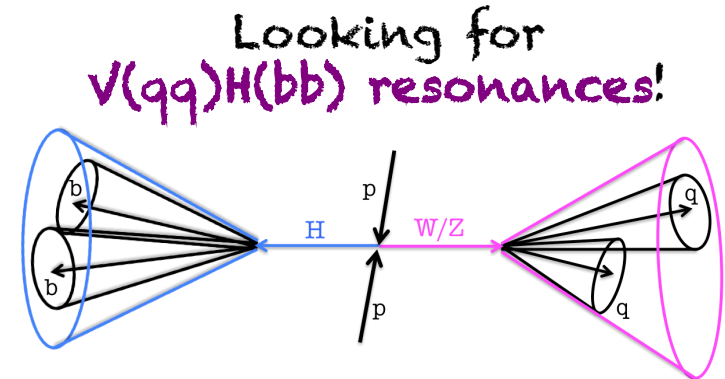


V(qq)H(bb) Search

Selection

- Large BRs: $W/Z \rightarrow qq$ (67%), $H \rightarrow bb$ (~70%).
- Select events with large-R jets consistent with highly boosted $V \rightarrow qq$ and $H \rightarrow bb$.

- Use **boson tagging**:
 - V-tagging: mass + $D_2^{\beta=1}$.
 - H-tagging: mass + b-tagging.



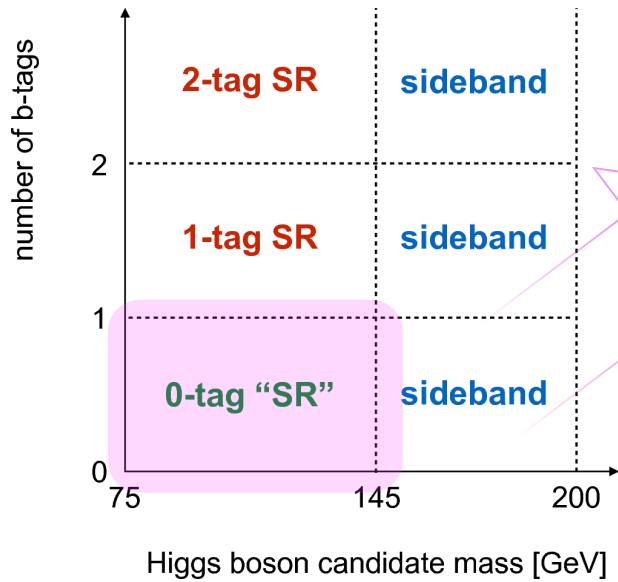
- Leading jet $p_T > 450$ GeV, sub-leading jet $p_T > 250$ GeV.
- Larger mass jet assigned as Higgs candidate.
- Events categorized in 1-tag and ≥ 2 -tag.
- **WH and ZH SRs not orthogonal** (~60% overlap).

V(qq)H(bb) Search

Strategy

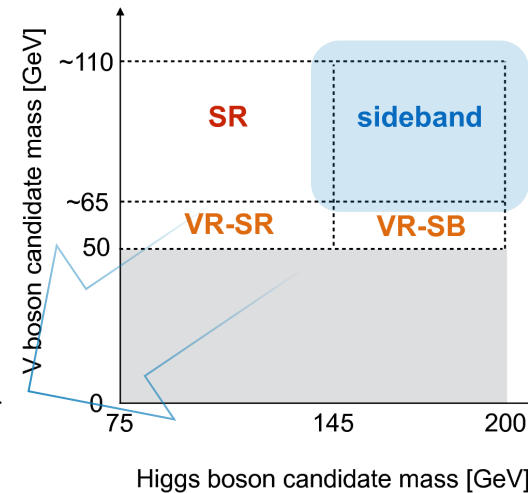
Main background from **multijet** events.

~10% contributions from t-tbar, ~1% from V+jets (taken from MC),



0-tag region in **data** is used to extract a template of the multijet background.

High mass side-bands used to extract normalization and re-weighting corrections.

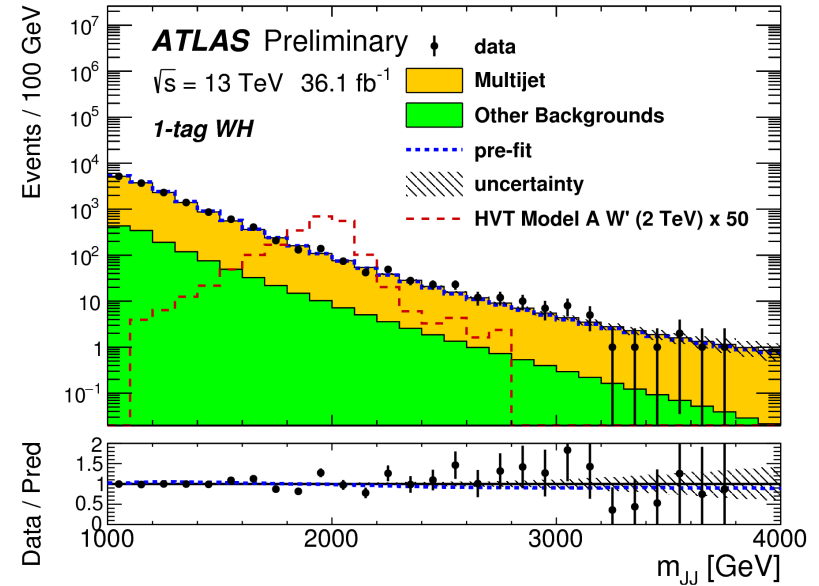
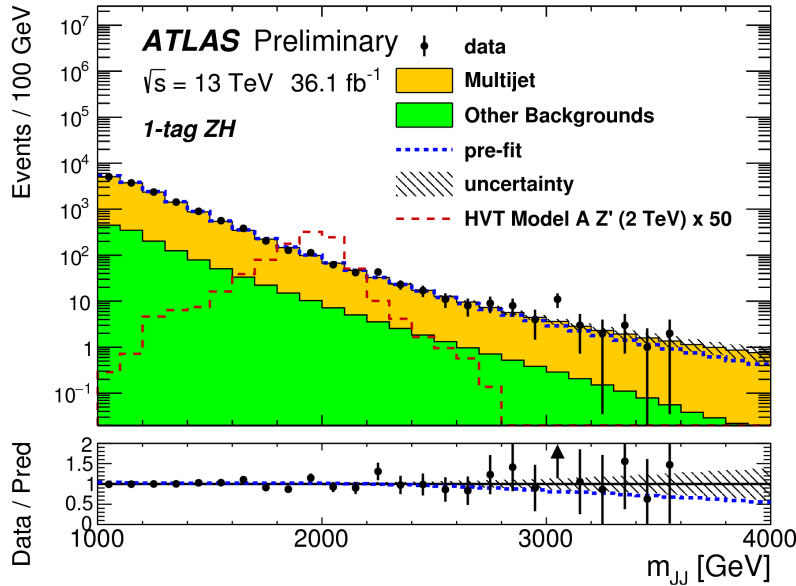


Multijet in SR

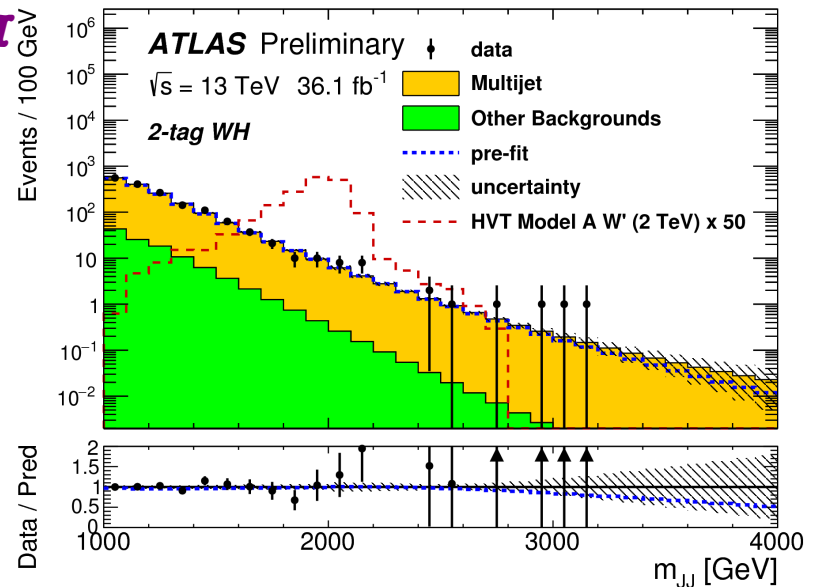
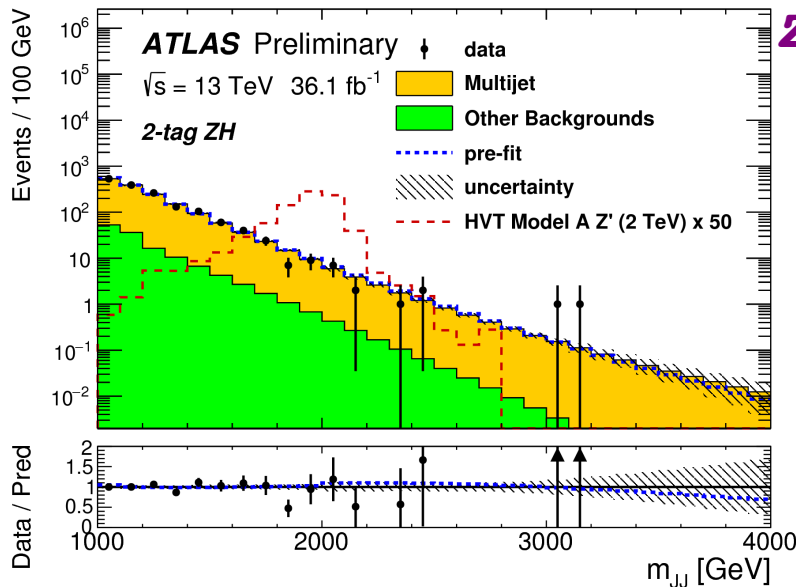
$$\mu_{\text{Multijet}}^{1(2)\text{-tag}} = \frac{N_{\text{Multijet}}^{1(2)\text{-tag}}}{N_{\text{Multijet}}^{0\text{-tag}}} = \frac{N_{\text{data}}^{1(2)\text{-tag}} - N_{t\bar{t}}^{1(2)\text{-tag}} - N_{V\text{+jets}}^{1(2)\text{-tag}}}{N_{\text{data}}^{0\text{-tag}} - N_{t\bar{t}}^{0\text{-tag}} - N_{V\text{+jets}}^{0\text{-tag}}}$$

Extract $\mu_{\text{multijets}}$ from high mass sideband, different for each SR: 1- and 2-tag, and WH, ZH.

V(qq)H(bb) Search

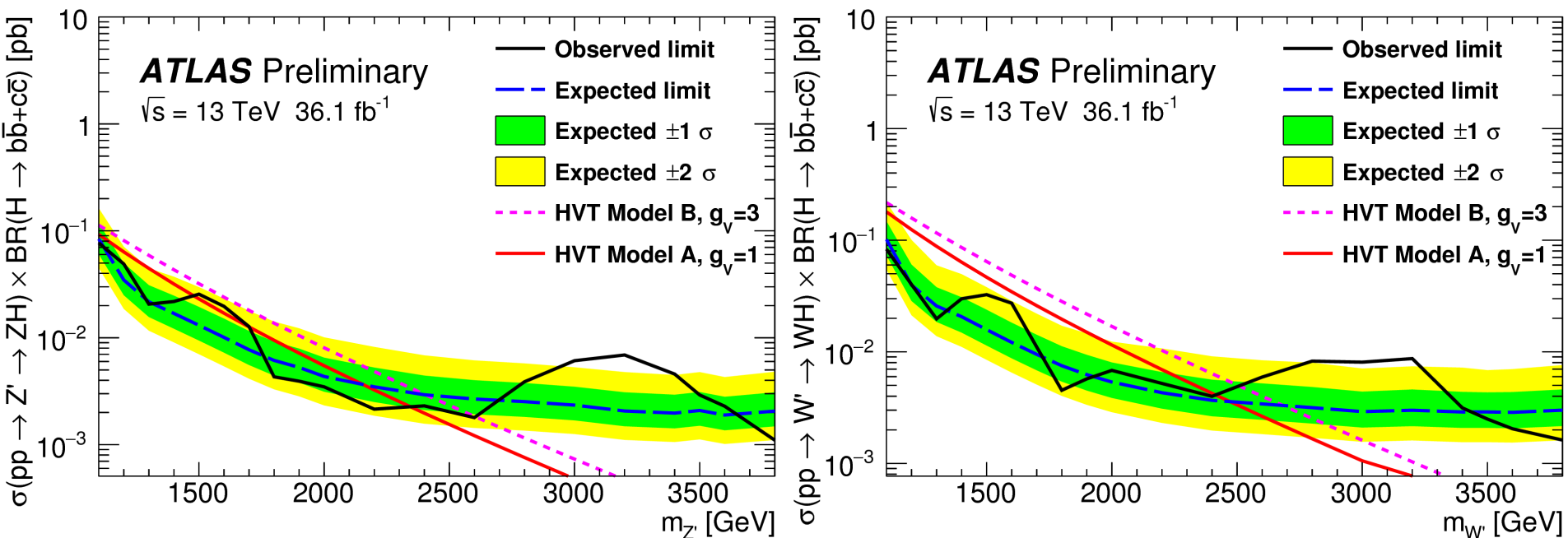


*Probing
ZH and WH
not orthogonal*



V(qq)H(bb) Search

- **Normalization and shape of multijet bkg:** estimated from largest deviation between data and prediction yields in validation region.
 - Normalization: 2-tag: 13%(sys), 3%(stat); 1-tag: 5% (sys), 1% (stat).
 - Shape (split for <2TeV and >2TeV).
- Fit **WH** and **ZH** signal regions separately.
 - Combining 1-tag and 2-tag regions in each case.

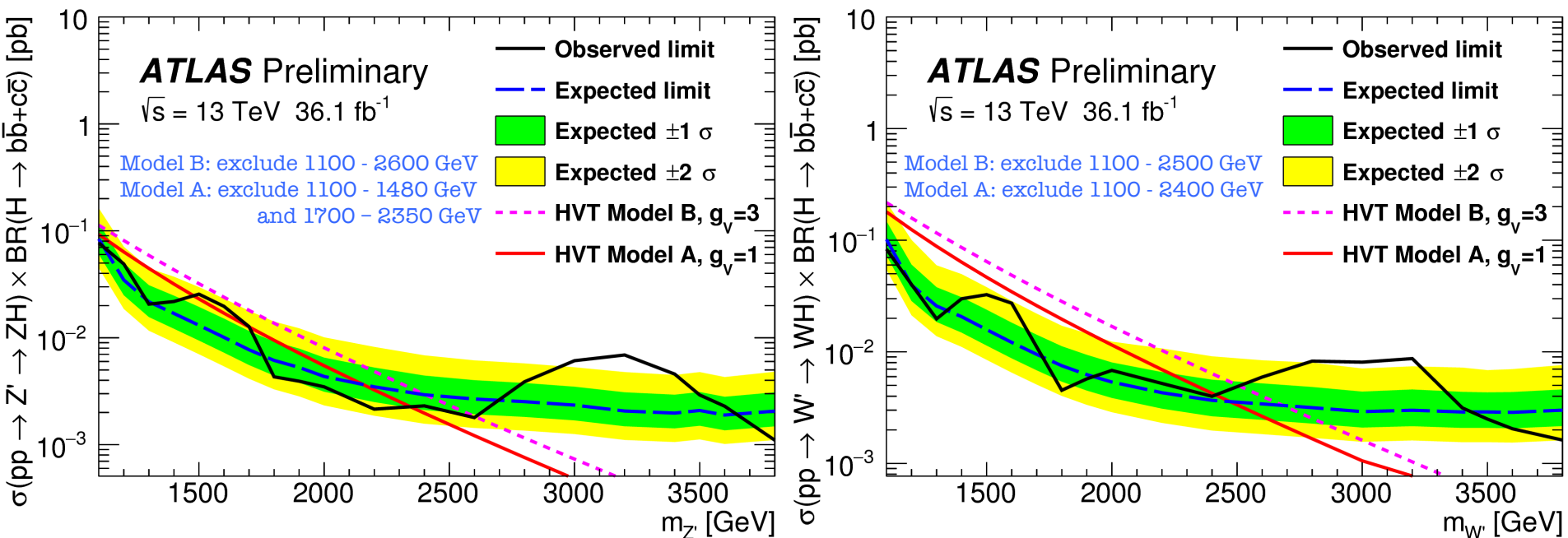


V(qq)H(bb) Search

Heavy Vector Triplet (HVT) W' and Z'.

- Model A: comparable BR to fermions and gauge bosons.
- Model B: Suppressed couplings to fermions.

Largest excess found at 3.0 TeV in ZH channel, with **global** significance of **2.2 σ** .



Dilepton Search

Run Number: 303499

Event Number: 959589792

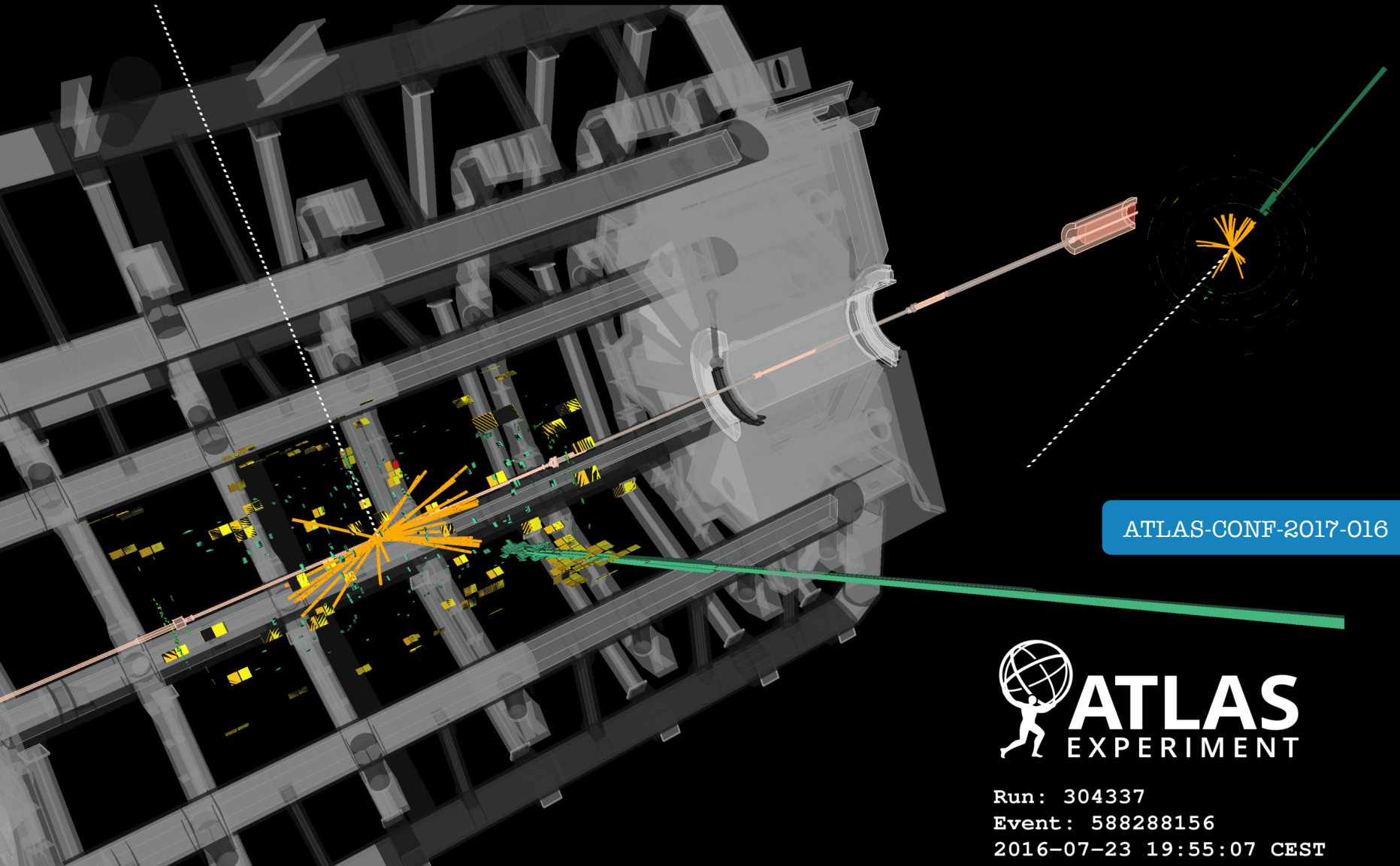
Date: 2016-07-08, 18:19:12 CET

ATLAS-CONF-2017-027



$m_{\mu\mu} = 1.98 \text{ TeV}$ invariant mass **di-muon event** observed with ATLAS

Lepton + E_T^{miss} Search



ATLAS-CONF-2017-016



Run: 304337
Event: 588288156
2016-07-23 19:55:07 CEST

Highest- m_T event in the **electron** channel observed with ATLAS: $m_T = 2.26 \text{ TeV}$
($p_T^e = 1.11 \text{ TeV}$, $E_T^{\text{miss}} = 1.16 \text{ TeV}$)

Searches with **Leptons**

Medium **Electrons**
Loose isolation

High p_T WP **Muons**
(Trk-based) Loose
isolation

- Single electron triggers.
- $E_T^{(\text{electron})} > 65 \text{ GeV}$.
- *Tight* ID.
- $m_T > 130 \text{ GeV}$.
- $E_T^{\text{miss}} > 65 \text{ GeV}$.
- Single muon triggers.
- $p_T^{(\text{muon})} > 55 \text{ GeV}$.
- $m_T > 110 \text{ GeV}$.
- $E_T^{\text{miss}} > 55 \text{ GeV}$.

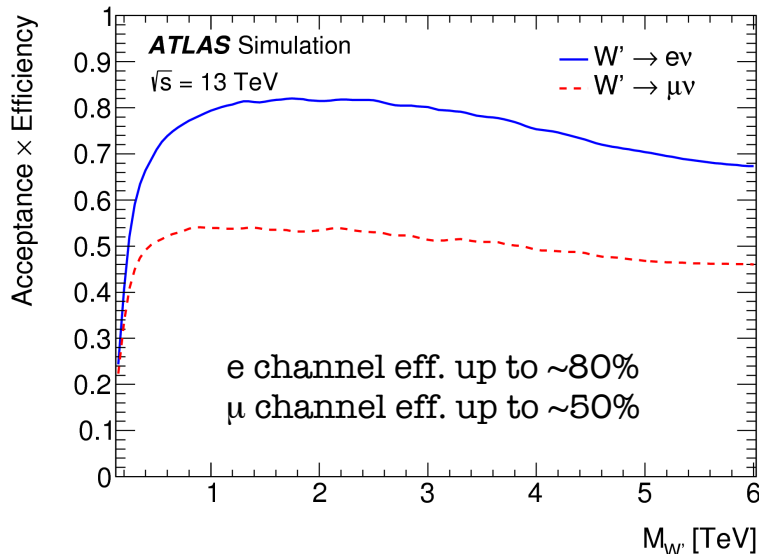
Veto on additional leptons

Lepton + E_T^{miss}

- Di-electron triggers.
- $E_T^{(\text{electrons})} > 30 \text{ GeV}$.
- Single muon triggers.
- $p_T^{(\text{muons})} > 30 \text{ GeV}$.

Highest $m_{\ell\ell}$ pair ($> 80 \text{ GeV}$).

Dilepton



- Reduced acceptance in the muon channels:
 - Lower *muon identification efficiency*,
 - *tighter selection criteria* (to improve muon resolution).
- Opposite charge required for *di-muons*.
 - Charge mis-identification does not affect energy measurement for electrons.

Strategy

Main background from **Drell-Yan production**.

Additional contributions from processes with **real leptons** in the final state (t-tbar, single top quark, diboson). *Estimated using MC samples.*

***DY** events are simulated with NLO Powheg generator. Events yields are corrected with mass dependent rescaling from NLO to NNLO QCD. Mass-dependent EW-corrections at NLO are also applied.*

- **Fakes** background: e.g. from multijet events, where one or more jets satisfies the lepton selection.
 - Negligible in muon channels. Minor background in the electron channels.
 - Using data-driven approach: **matrix method**. Measure fake and real rates: probabilities of a jet or an electron **to be identified as an electron**.

Background estimates may suffer from low statistics in the high mass tails (e.g. multijets). Extrapolation performed by fitting the lower mass distribution and using the fitted function to predict the background at higher mass.

Dilepton Search

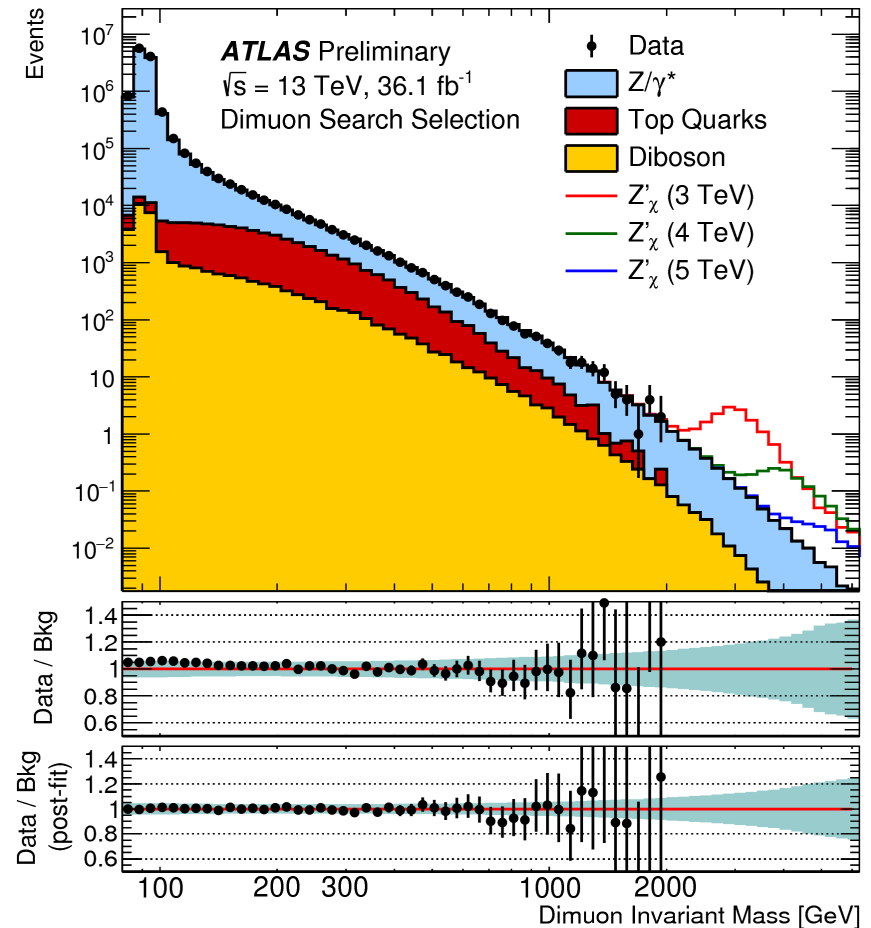
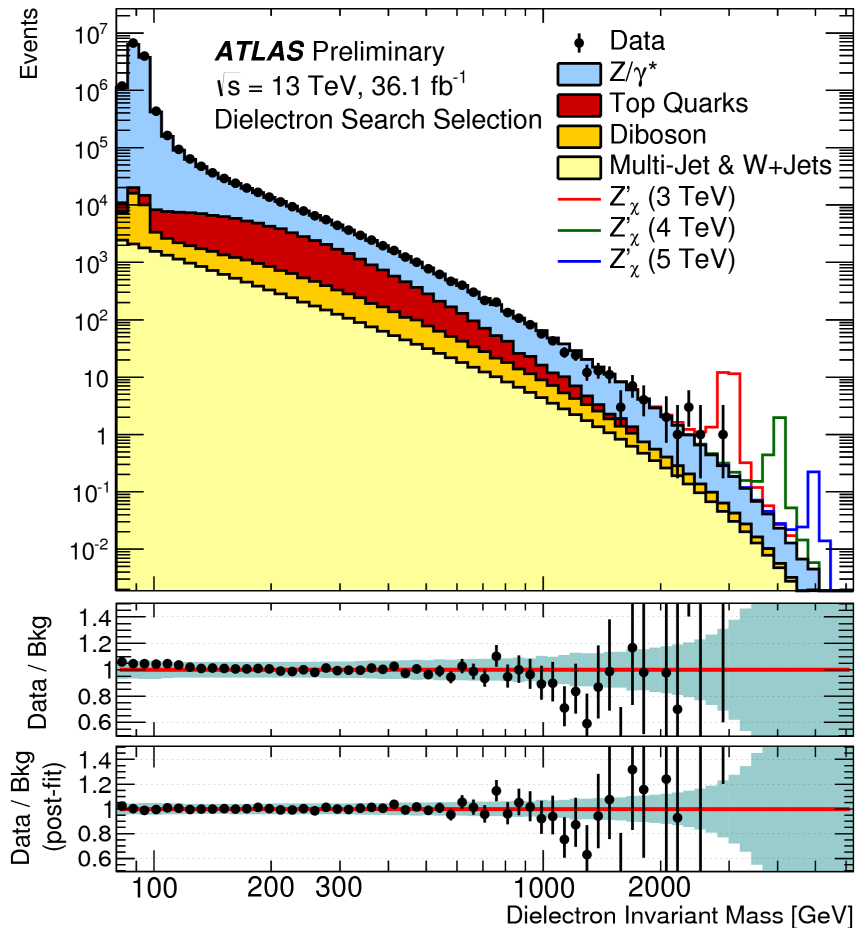
Source	Dielectron channel		Dimuon channel	
	Signal	Background	Signal	Background
Luminosity	3.2% (3.2%)	3.2% (3.2%)	3.2% (3.2%)	3.2% (3.2%)
MC statistical	<1.0% (<1.0%)	<1.0% (<1.0%)	<1.0% (<1.0%)	<1.0% (<1.0%)
Beam energy	2.0% (4.1%)	2.0% (4.1%)	1.9% (3.1%)	1.9% (3.1%)
Pile-Up effects	<1.0% (<1.0%)	<1.0% (<1.0%)	<1.0% (<1.0%)	<1.0% (<1.0%)
DY PDF choice	N/A	<1.0% (8.4%)	N/A	<1.0% (1.9%)
DY PDF variation	N/A	8.7% (19%)	N/A	7.7% (13%)
DY PDF scale	N/A	1.0% (2.0%)	N/A	<1.0% (1.5%)
DY α_S	N/A	1.6% (2.7%)	N/A	1.4% (2.2%)
DY EW corrections	N/A	2.4% (5.5%)	N/A	2.1% (3.9%)
DY γ -induced corrections	N/A	3.4% (7.6%)	N/A	3.0% (5.4%)
Top Quarks theoretical	N/A	<1.0% (<1.0%)	N/A	<1.0% (<1.0%)
Dibosons theoretical	N/A	<1.0% (<1.0%)	N/A	<1.0% (<1.0%)
Reconstruction efficiency	<1.0% (<1.0%)	<1.0% (<1.0%)	10% (17%)	10% (17%)
Isolation efficiency	9.1% (9.7%)	9.1% (9.7%)	1.8% (2.0%)	1.8% (2.0%)
Trigger efficiency	<1.0% (<1.0%)	<1.0% (<1.0%)	<1.0% (<1.0%)	<1.0% (<1.0%)
Identification efficiency	2.6% (2.4%)	2.6% (2.4%)	N/A	N/A
Lepton energy scale	<1.0% (<1.0%)	4.1% (6.1%)	<1.0% (<1.0%)	<1.0% (<1.0%)
Lepton energy resolution	<1.0% (<1.0%)	<1.0% (<1.0%)	2.7% (2.7%)	<1.0% (6.7%)
Multi-jet & W +jets	N/A	10% (129%)	N/A	N/A
Total	10% (11%)	18% (132%)	11% (18%)	14% (24%)

Largest theory uncertainty.

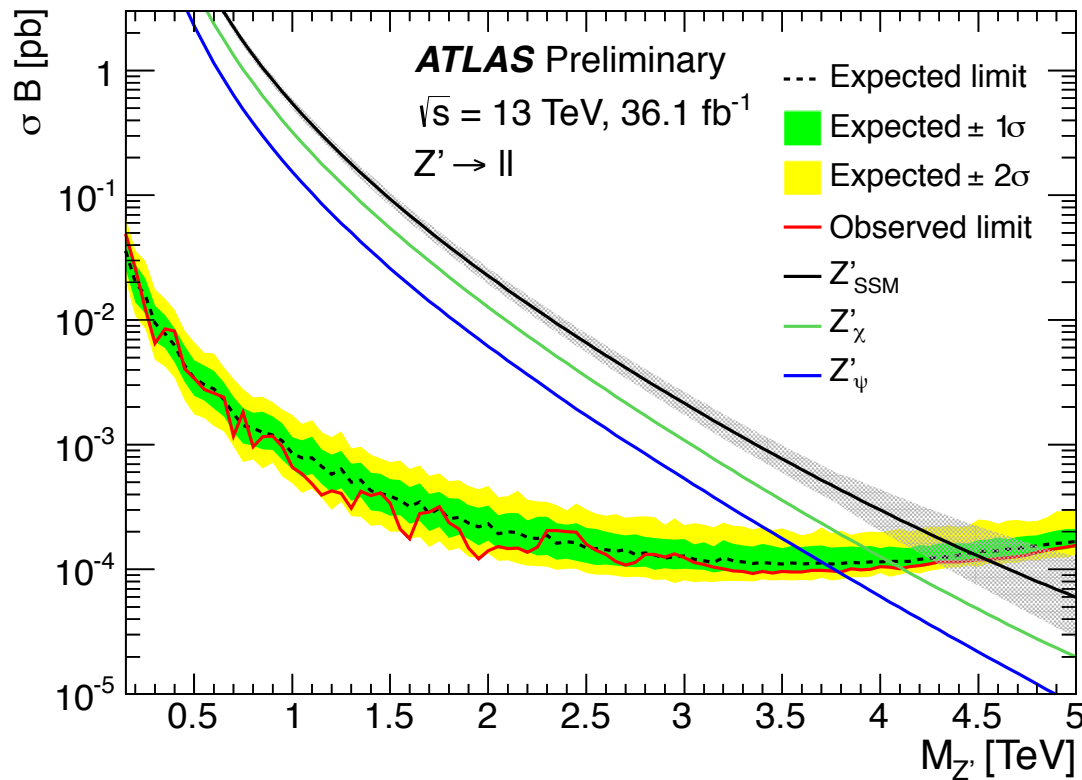
Largest exp uncertainty.

Large uncertainty at high masses due to extrapolation.

Background and signal systematic uncertainties at dilepton masses of 2 TeV (4 TeV).



○ Most significant excess in di-electron mass spectrum is observed at 2.37 TeV, global significance of -0.2σ .



Limits

Upper limits are set for Z' cross sections times BR wrt $m_{Z'}$, for various Z' scenarios.

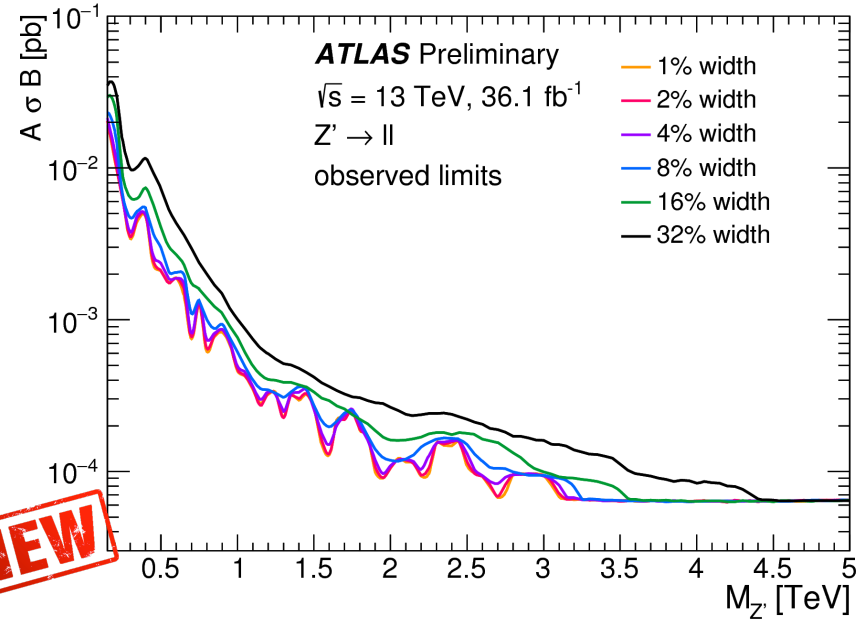
*Limits weaken above 3.5 TeV:
 Rapidly falling signal x-sections and
 off-shell low mass signal tail.*

Model	Width [%]	θ_{E_6} [Rad]	Lower limits on $m_{Z'}$ [TeV]					
			ee		$\mu\mu$		$\ell\ell$	
			Obs	Exp	Obs	Exp	Obs	Exp
Z'_{SSM}	3.0	-	4.3	4.3	4.0	3.9	4.5	4.5
Z'_χ	1.2	0.50π	3.9	3.9	3.6	3.6	4.1	4.0
Z'_S	1.2	0.63π	3.9	3.8	3.6	3.5	4.0	4.0
Z'_I	1.1	0.71π	3.8	3.8	3.5	3.4	4.0	3.9
Z'_η	0.6	0.21π	3.7	3.7	3.4	3.3	3.9	3.8
Z'_N	0.6	-0.08π	3.6	3.6	3.4	3.3	3.8	3.8
Z'_ψ	0.5	0π	3.6	3.6	3.3	3.2	3.8	3.7

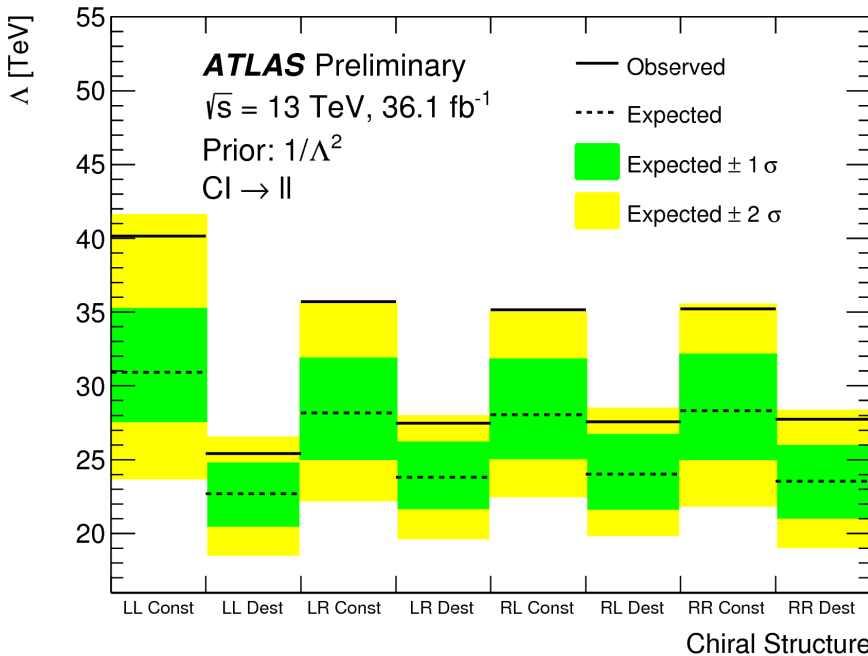
Limits for minimal Z' models are also discussed in the paper.

Generic Z' limits

Aim to provide more general limits.
 Applying fiducial cuts ($p_T > 30$ GeV, $|\eta| < 2.5$)
 on signal templates and a mass window of ± 2
 the signal width (Breit-Wigner).
*Other models can be interpreted
 with these cross-sections!*



NEW

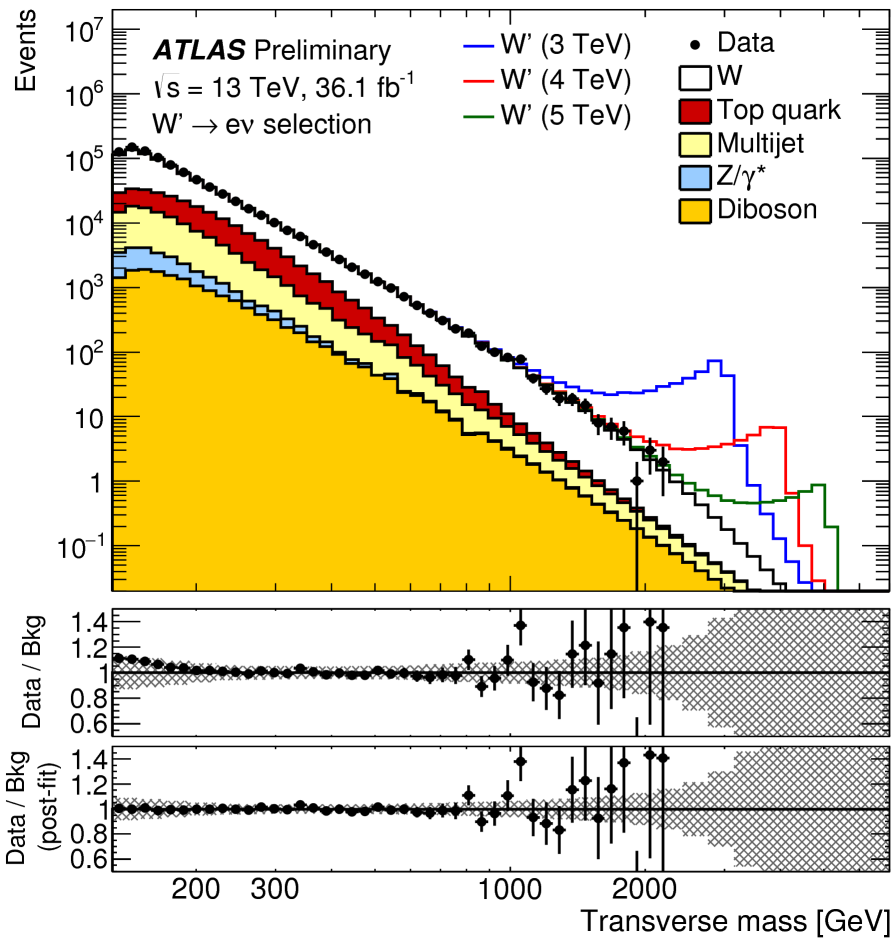


CI Limits

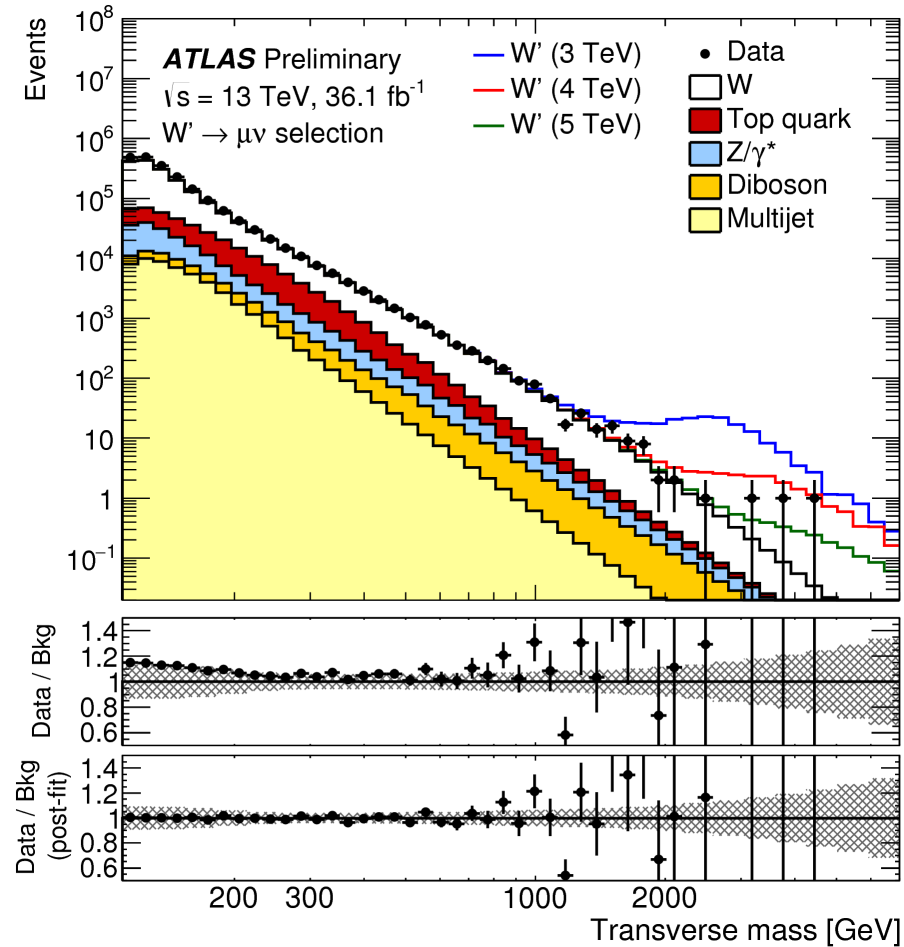
$$\mathcal{L} = \frac{g^2}{\Lambda^2} [\eta_{LL} (\bar{q}_L \gamma_\mu q_L) (\bar{\ell}_L \gamma^\mu \ell_L) + \eta_{RR} (\bar{q}_R \gamma_\mu q_R) (\bar{\ell}_R \gamma^\mu \ell_R) + \eta_{LR} (\bar{q}_L \gamma_\mu q_L) (\bar{\ell}_R \gamma^\mu \ell_R) + \eta_{RL} (\bar{q}_R \gamma_\mu q_R) (\bar{\ell}_L \gamma^\mu \ell_L)]$$

Different chiral structures are studied;
 with the left-right (right-left) model
 obtained by setting $\eta_{LR} = \pm 1$ ($\eta_{RL} = \pm 1$)
 and all other parameters to zero.

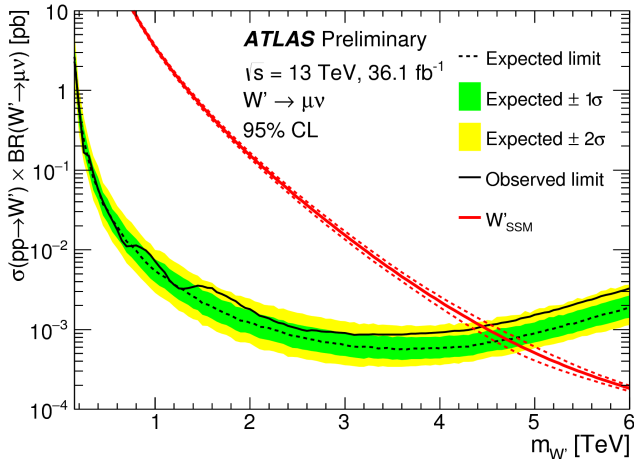
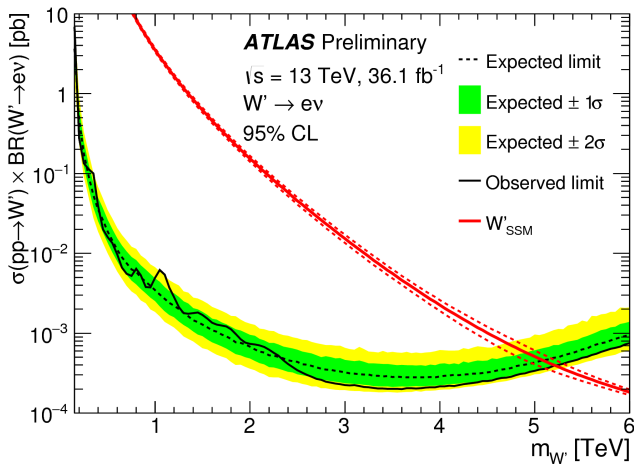
Lepton + E_T^{miss} Search



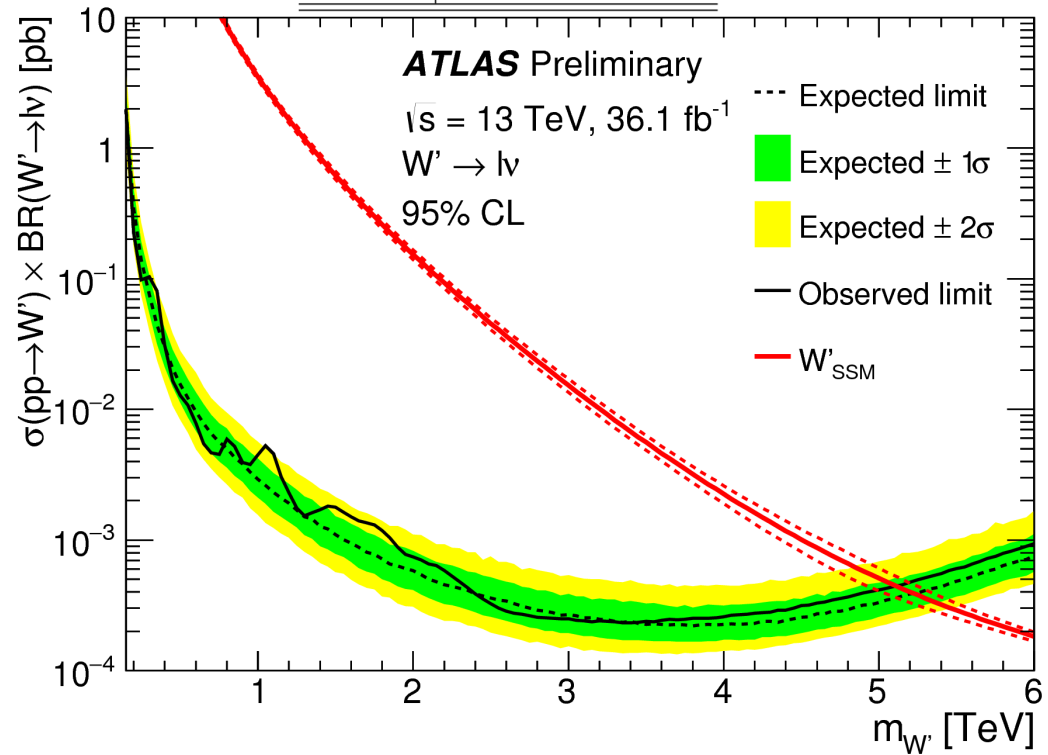
○ Most significant excess in electron channel is at $m_{W'} = 1.1 \text{ TeV}$, global significance of 0.6σ .



○ Most significant excess in muon channel is at $m_{W'} \sim 5 \text{ TeV}$, global significance of 0.1σ .



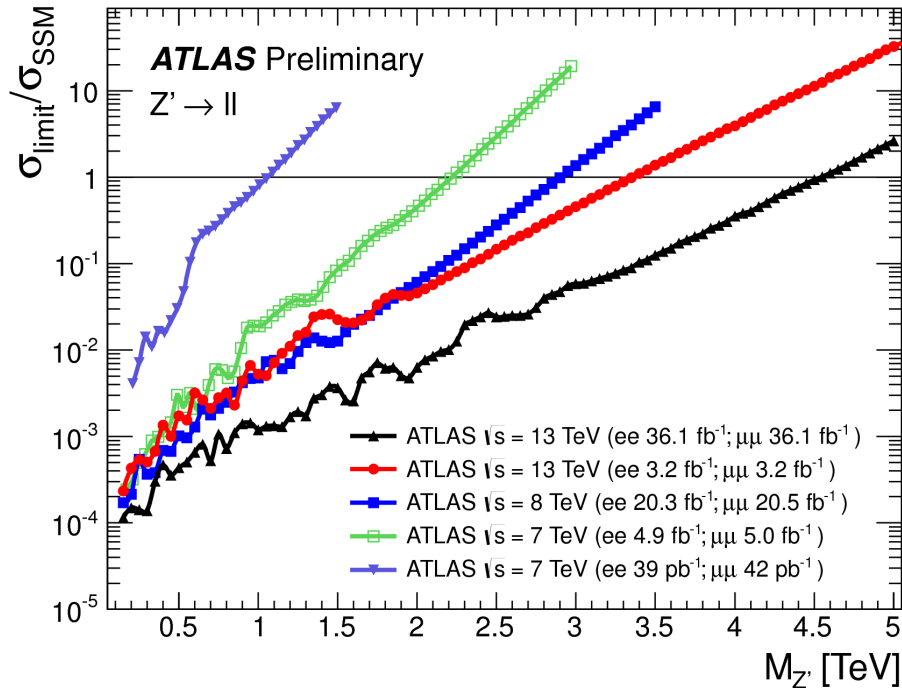
Decay	$m_{W'}$ lower limit [TeV]	
	Expected	Observed
$W' \rightarrow e\nu$	5.09	5.22
$W' \rightarrow \mu\nu$	4.70	4.45
$W' \rightarrow \ell\nu$	5.22	5.11



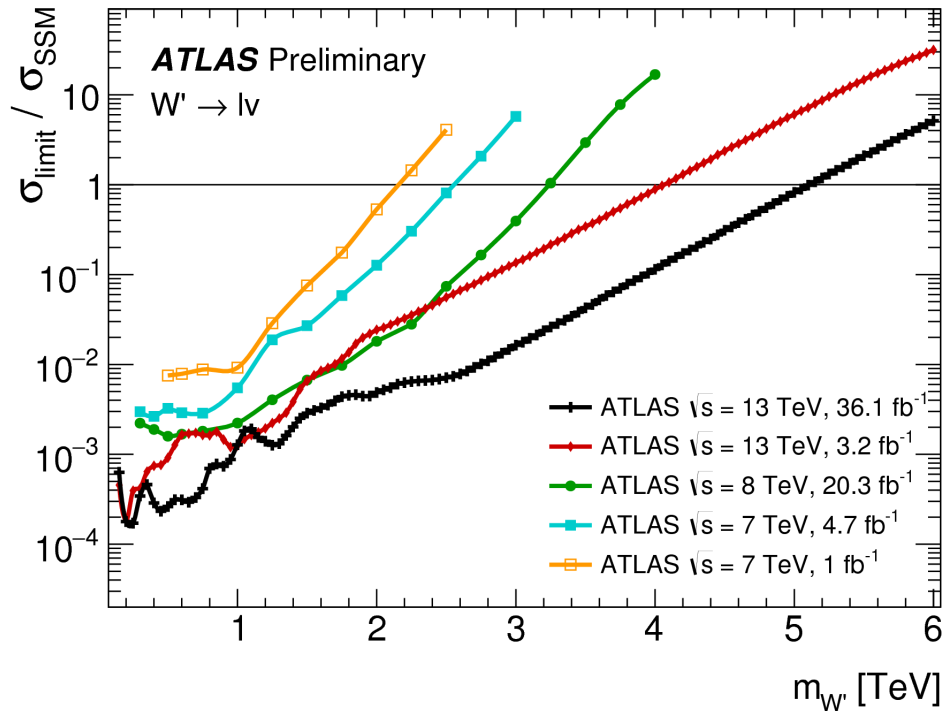
- Combination of the two channels
 - Uncertainties treated as correlated.
- Stronger expected limits from electron channel.
 - Larger acceptance times efficiency,
 - better momentum resolution.

Upper limits on cross section times BR for the electron and muon channels.

Significant improvement wrt previous ATLAS searches!



Observed limits to the Z'_{SSM} cross section from the combination of di-electron and di-muon channels.



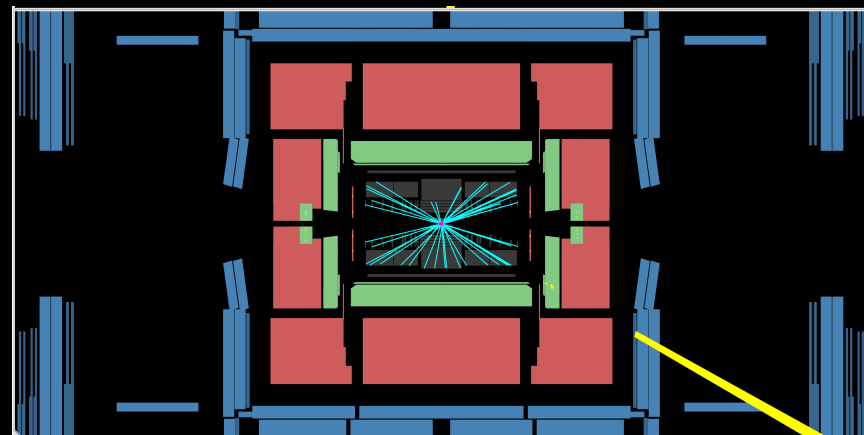
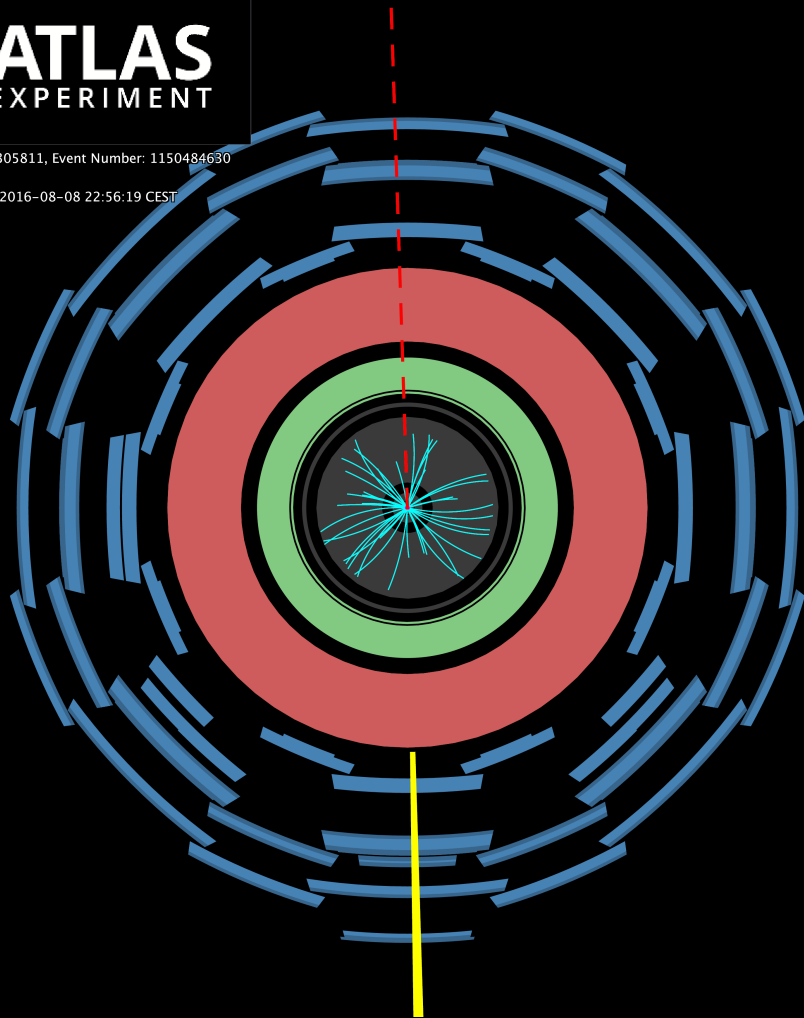
Observed limits to the W'_{SSM} cross section from the combination of electron and muon channels.

Photon + E_T^{miss} Search



Run Number: 305811, Event Number: 1150484630

Date: 2016-08-08 22:56:19 CEST



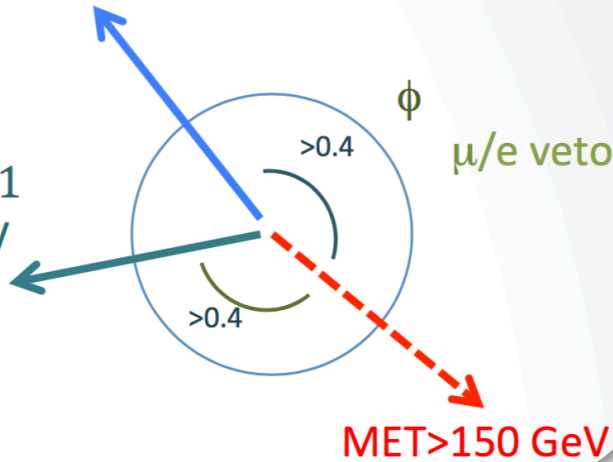
[arxiv:1704.03848](https://arxiv.org/abs/1704.03848)

A photon with $E_T = 265$ GeV is balanced by E_T^{miss} of 268 GeV.

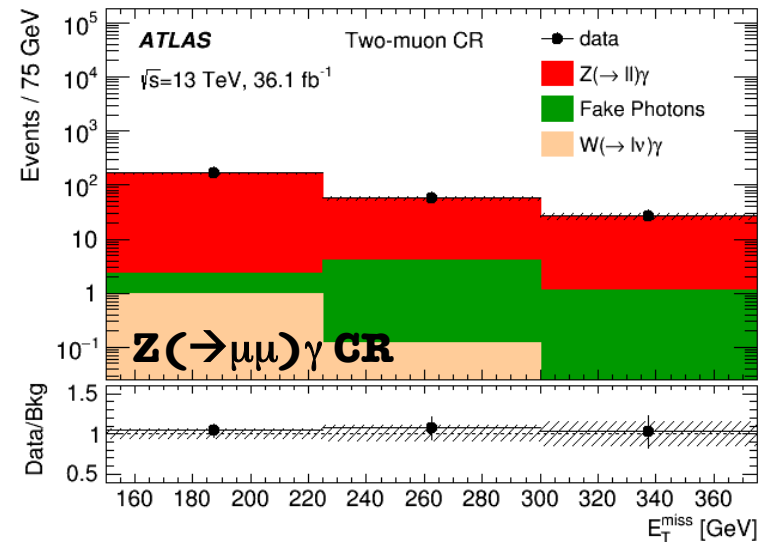
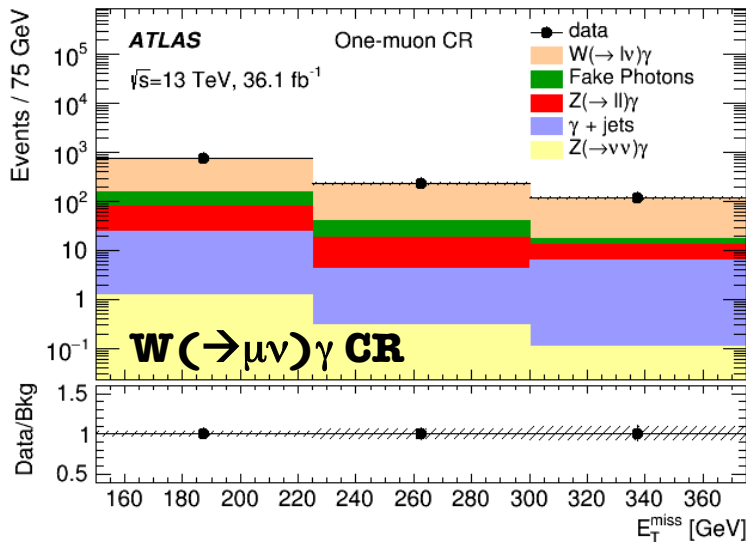
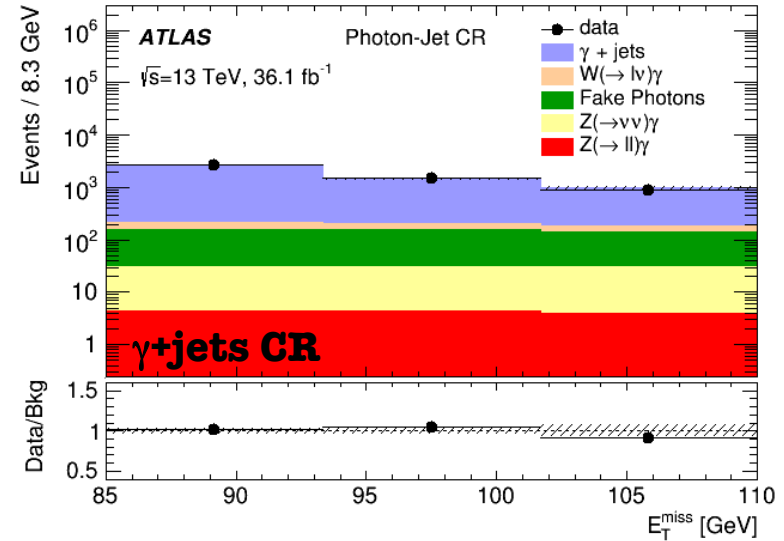
Selection

γ : $p_{T\gamma} > 150$ GeV,

jet: up to 1
 $p_T > 30$ GeV

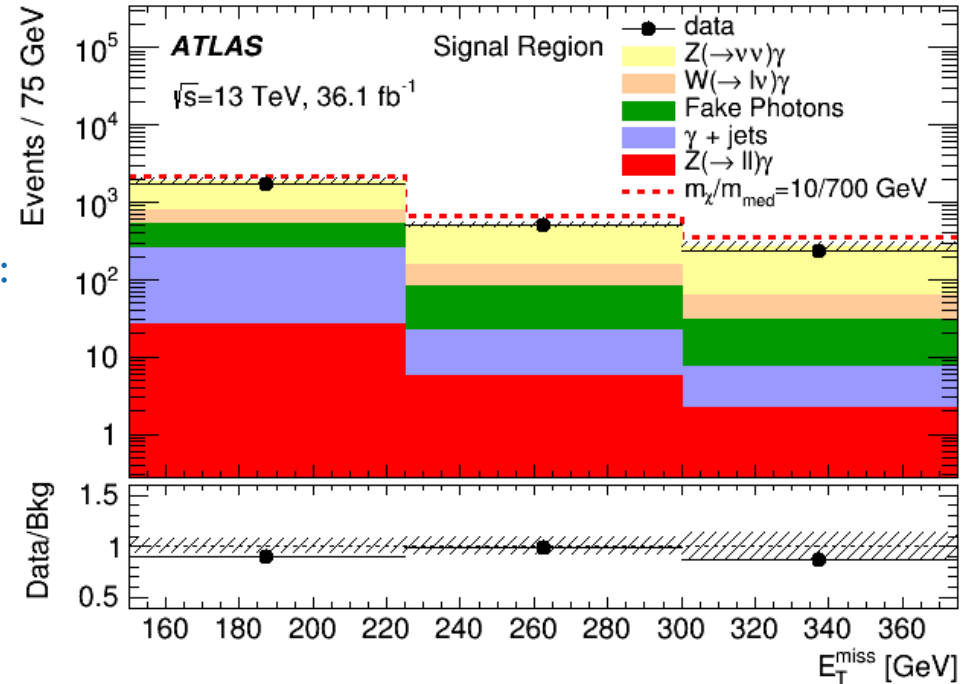
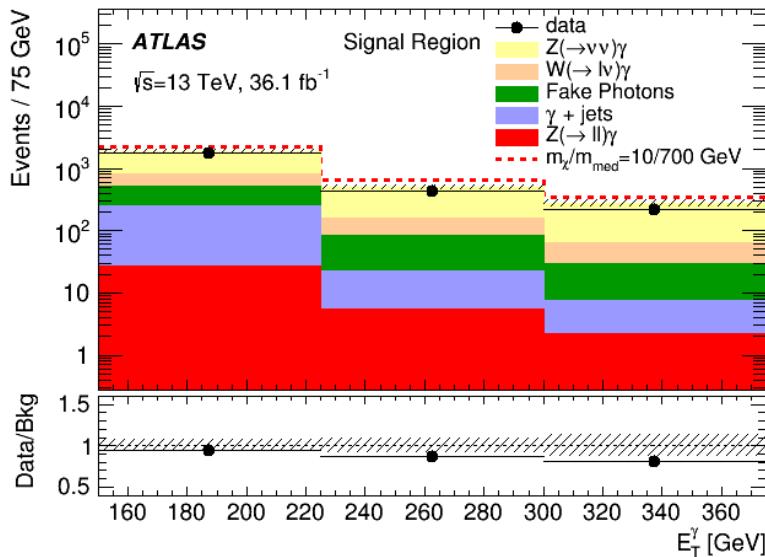


Multiple CRs defined to constrain SM bkg's



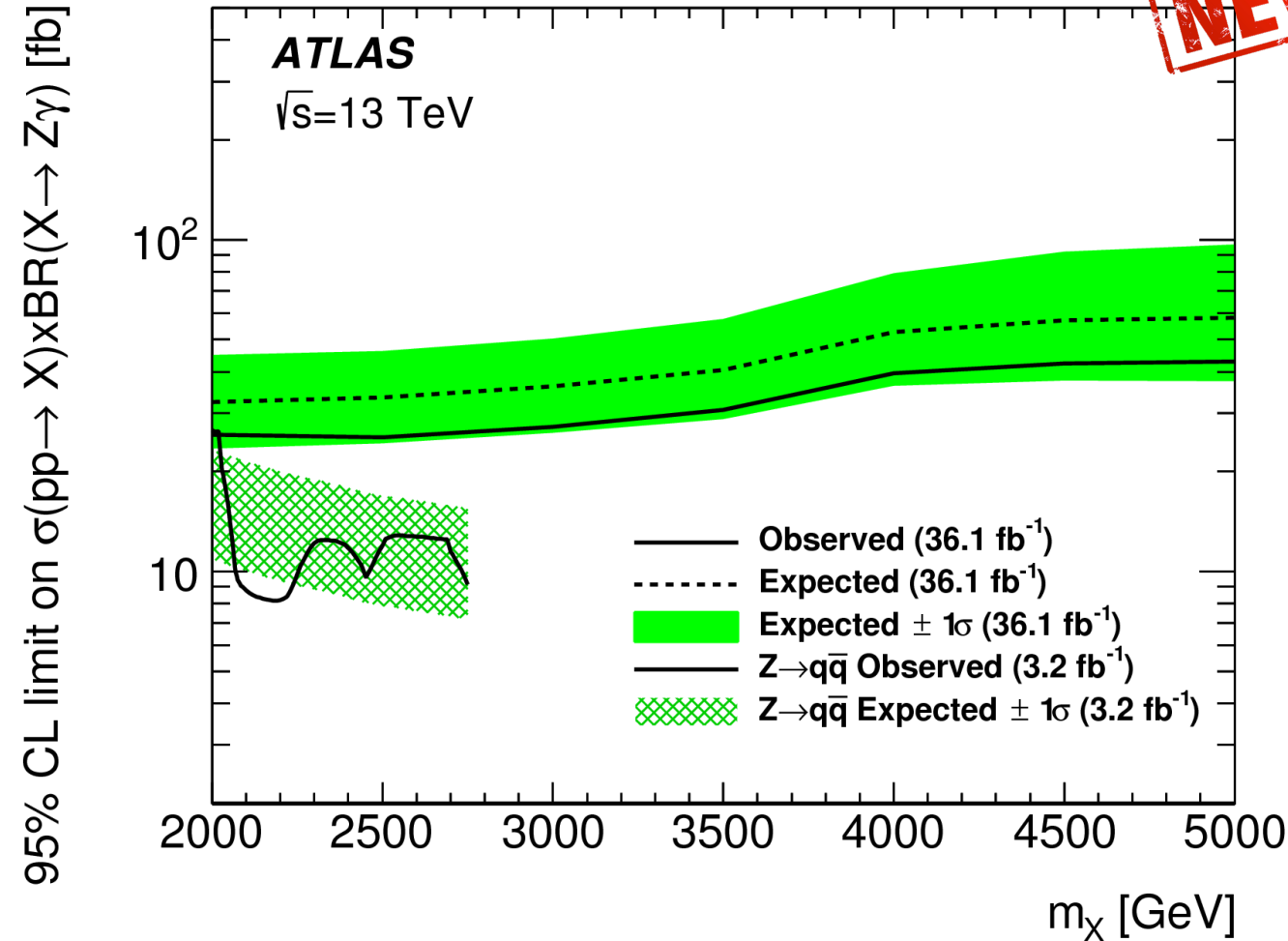
Strategy

- Dominant: $Z(\nu\nu) + \gamma$ (ISR), followed by $W\gamma$ and fake γ .
- $V\gamma$ +jets normalized in dedicated CRs.
- NEW** ○ 3 E_T^{miss} dependent scale factors: k_Z, k_W, k_{jet} .
 - $Z(\nu\nu)$ normalized in $2\mu + 2e$ CRs.
 - γ +jets bkg from γ +jet CR.



Main uncertainties: Statistical from CRs: 9%.

This analysis places limits on simplified DM models (photon from ISR) and EFT DM models (probing the $\gamma\gamma\chi$ coupling).



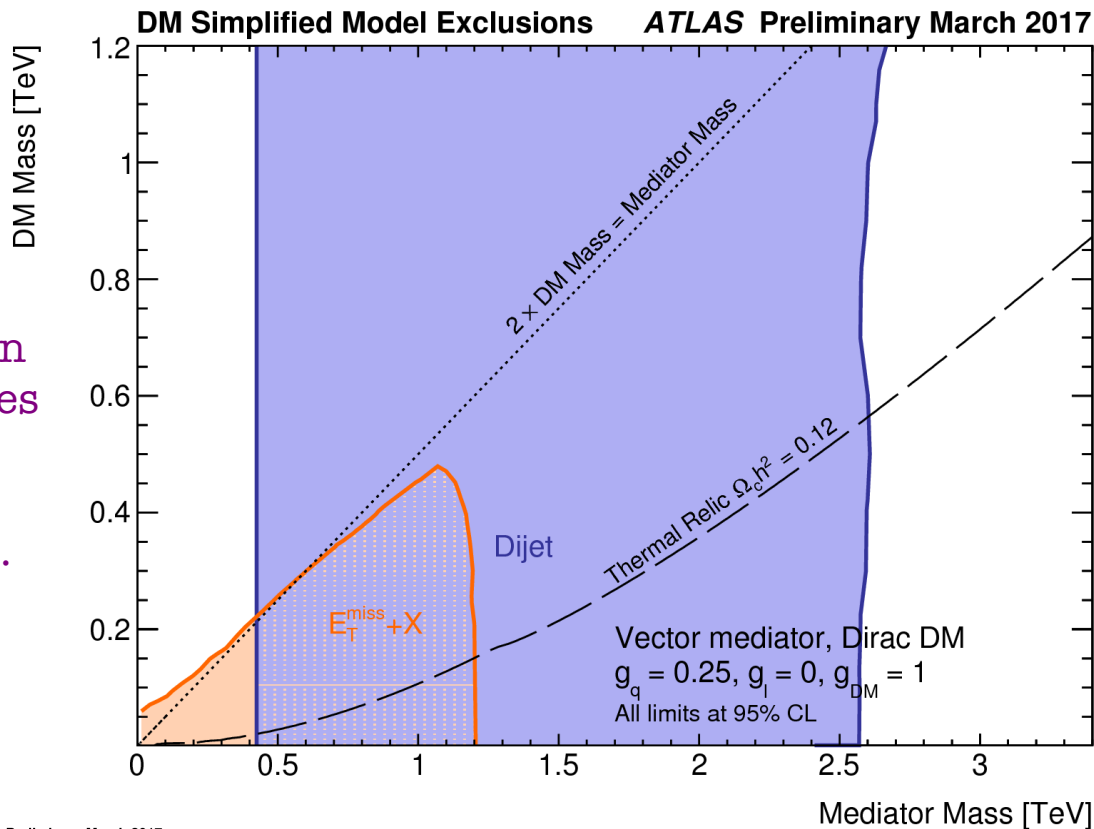
New results for
 $Z(\nu\nu)\gamma$ resonance
as a function of its mass.

Limits from **$Z(qq)\gamma$** with
 3.2 fb^{-1} are shown for
comparison.

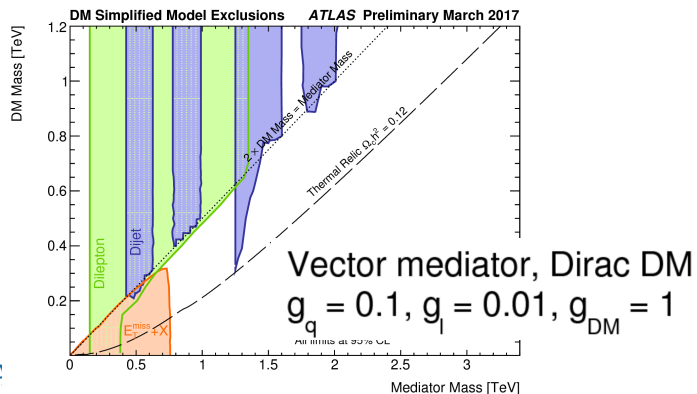
BONUS!

Connection to Dark Matter

Di-jet and dilepton resonance searches interpreted in terms of DM mediators limits.



- Dijet**
 Dijet 8 TeV $\sqrt{s} = 8 \text{ TeV}$, 20.3 fb⁻¹
 Phys. Rev. D. 91 052007 (2015)
 Dijet $\sqrt{s} = 13 \text{ TeV}$, 37.0 fb⁻¹
 arXiv:1703.09127 [hep-ex]
 Dijet TLA $\sqrt{s} = 13 \text{ TeV}$, 3.4 fb⁻¹
 ATLAS-CONF-2016-030
- $E_T^{\text{miss}} + X$**
 $E_T^{\text{miss}} + \gamma$ $\sqrt{s} = 13 \text{ TeV}$, 36.4 fb⁻¹
 CERN-EP-2017-044
- Dilepton**
 $\sqrt{s} = 13 \text{ TeV}$, 36.1 fb⁻¹
 ATLAS-CONF-2017-027



*However, note that the **choice of couplings** is very relevant to study the complementarity of these and other mono-X searches.*

Conclusions

- Searches for new physics have been performed with the full 2015+2016 dataset.
 - **Not possible to achieve without the amazing performance of the LHC machine and injector chain. Thanks to all involved!**
- New resonances and contact interactions are a strong components of the LHC physics program.
 - New techniques are being developed and new models are studied.
 - *So far, no significant deviations from Standard Model observed.*
 - Improved limits on multiple signal models!
 - Di-jet searches now exclude excited quarks up to 6 TeV.
 - Upper limits on $\sigma \times \text{BR}$ to the $q\bar{q}(\gamma)bb$ final state are set for masses between 1.1-3.8 TeV.
 - W'_{SSM} excluded for $m_{W'} > 5.1$ TeV from the lepton + $E_{\text{T}}^{\text{miss}}$ search,
 - Z'_{SSM} excluded for $m_{Z'} > 4.5$ TeV from di-lepton searches.
 - Upper limits on $\sigma \times \text{BR}$ for a $Z(\nu\nu)\gamma$ resonance set for masses between 2-5 TeV.

Di-Jet	arXiv:1703.09127
V(qq)H(bb)	ATLAS-CONF-2017-018
Dilepton	ATLAS-CONF-2017-027
Lepton + $E_{\text{T}}^{\text{miss}}$	ATLAS-CONF-2017-016
Photon + $E_{\text{T}}^{\text{miss}}$	arXiv:1704.03848



Many thanks!

Bonus Slides

ATLAS Detector

Muons Spectrometer

MS includes precision tracking chambers ($|\eta| < 2.7$) and fast detectors for triggering ($|\eta| < 2.4$).

Trigger

Hardware based L1 $\sim 100\text{kHz}$
Software based HLT $\sim 1\text{kHz}$

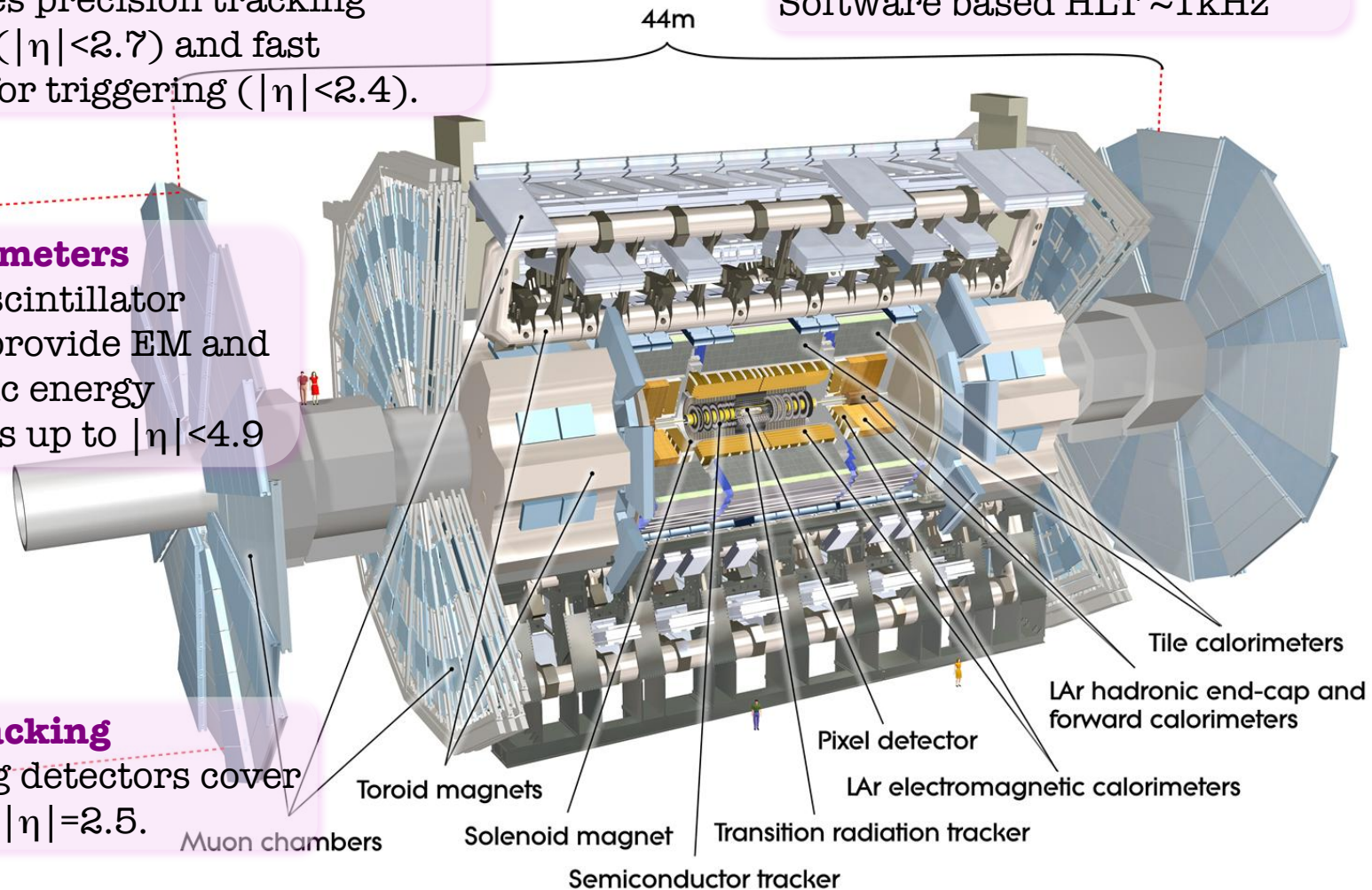
Calorimeters

LAr and scintillator calorimeters provide EM and hadronic energy measurements up to $|\eta| < 4.9$

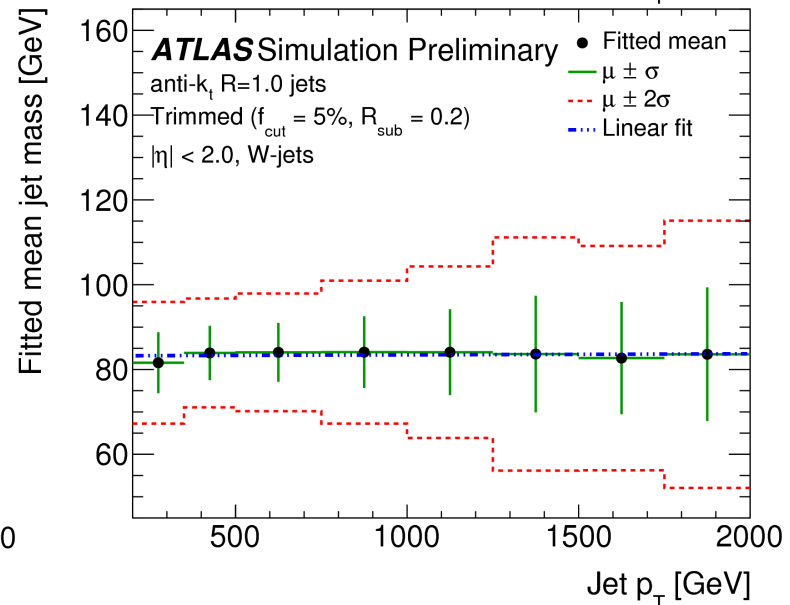
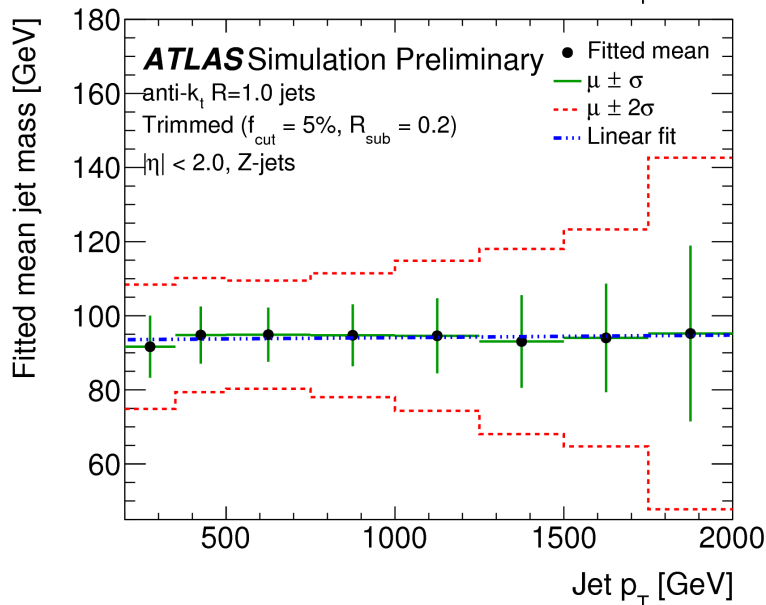
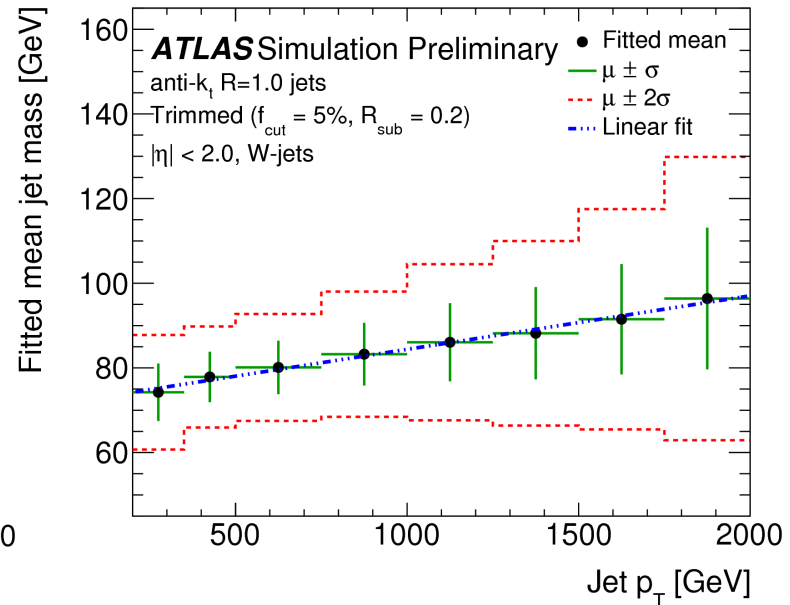
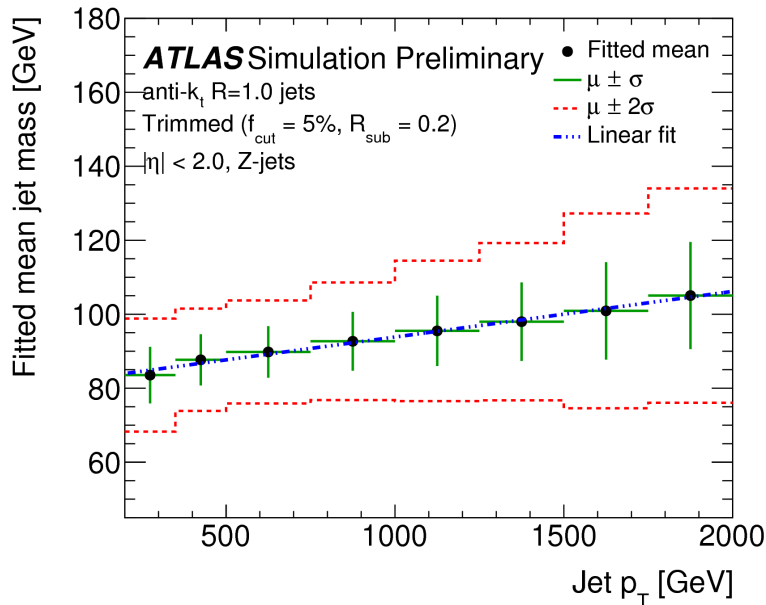
25m

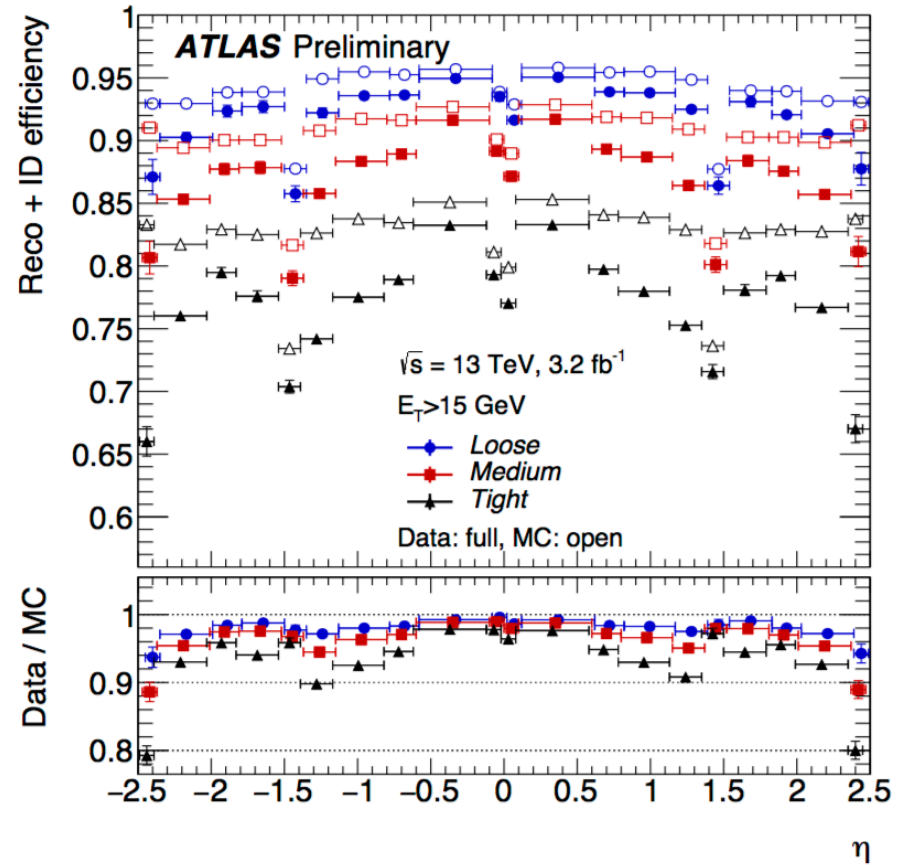
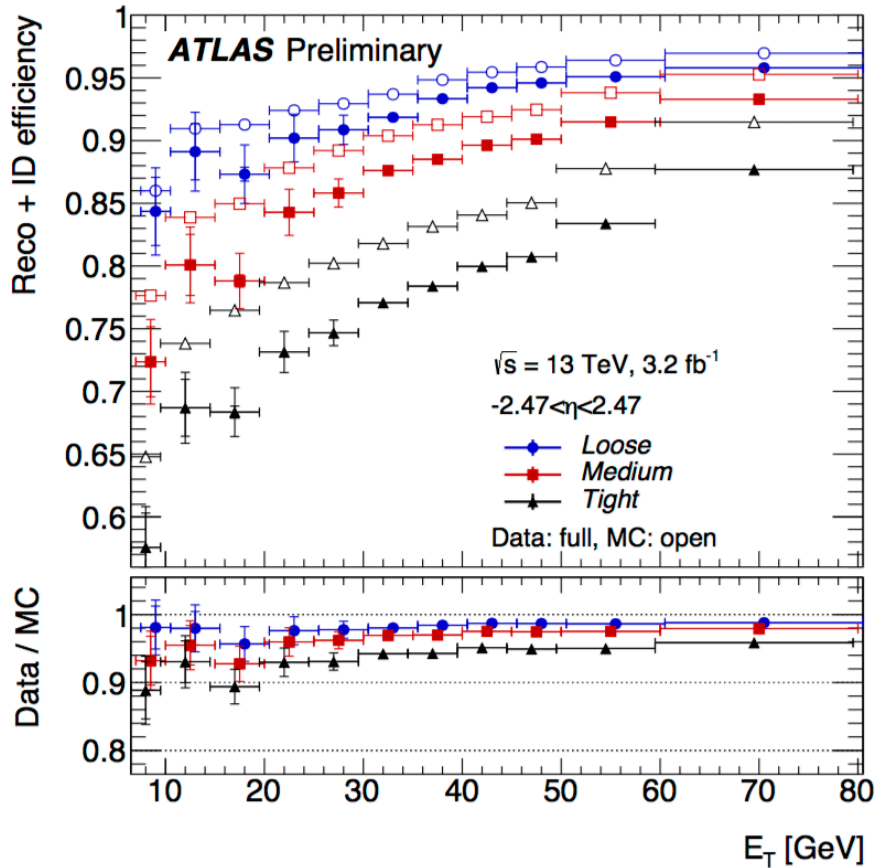
Tracking

Inner tracking detectors cover up to $|\eta| = 2.5$.

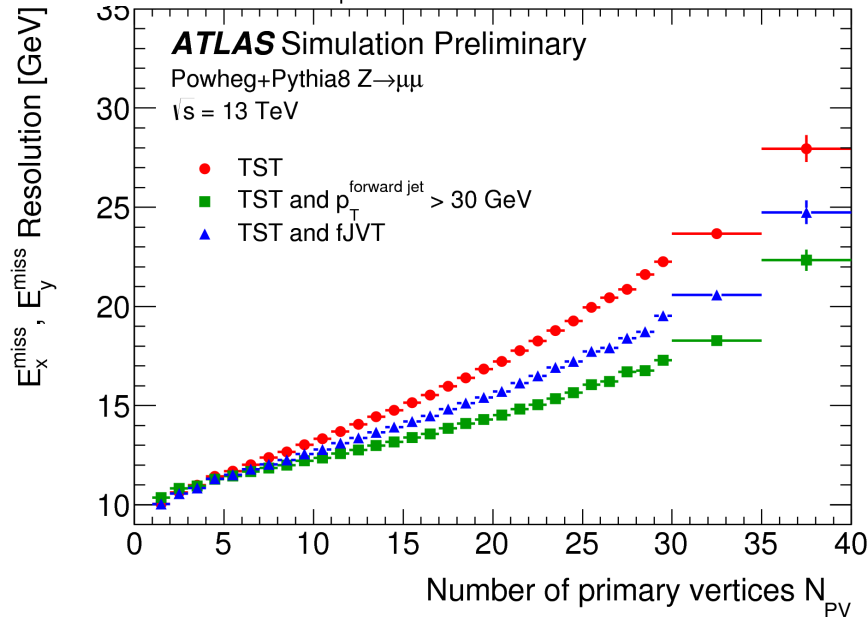
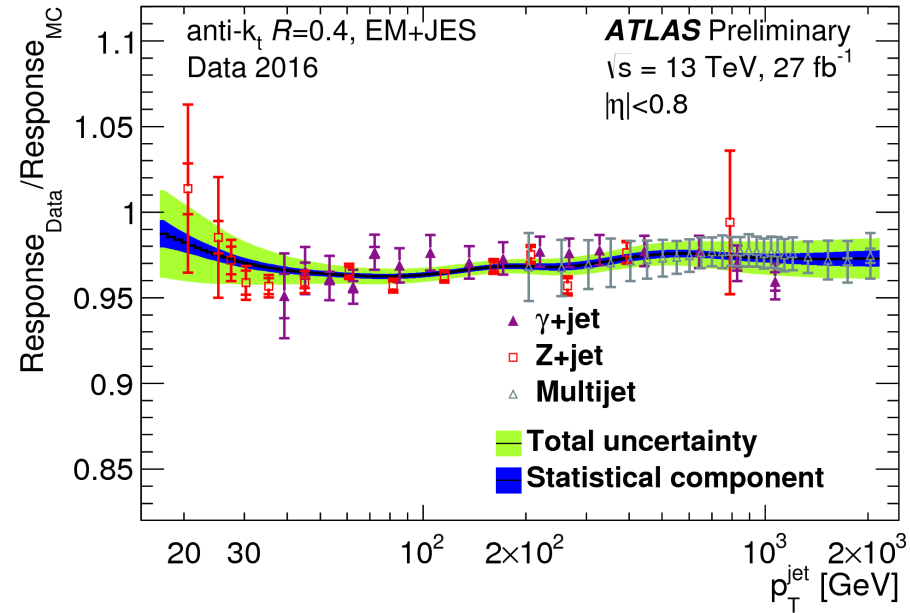
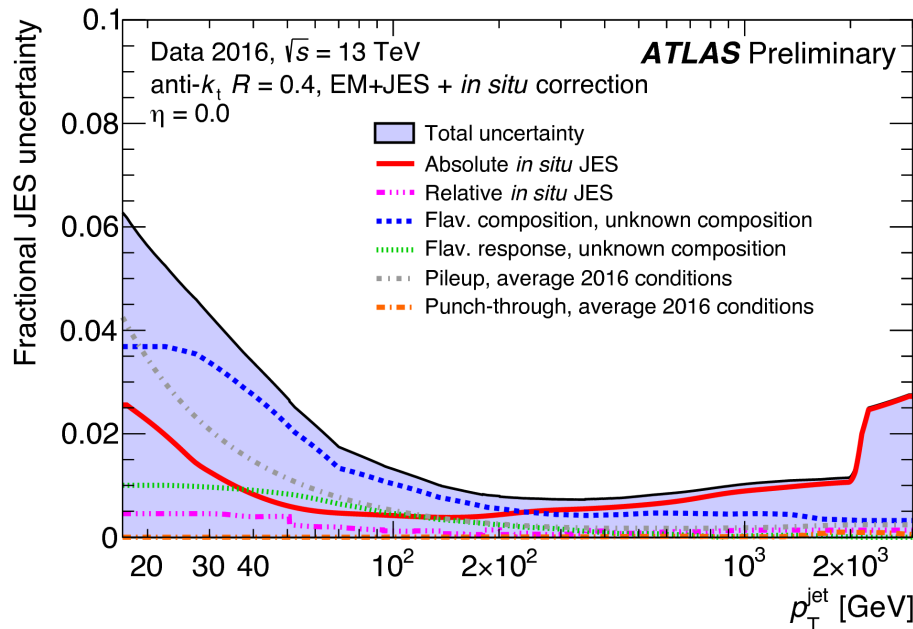


Performance: *Boson Tagging*





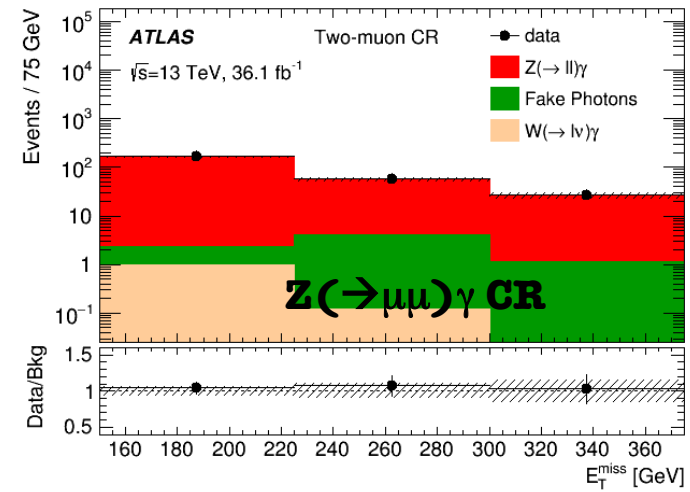
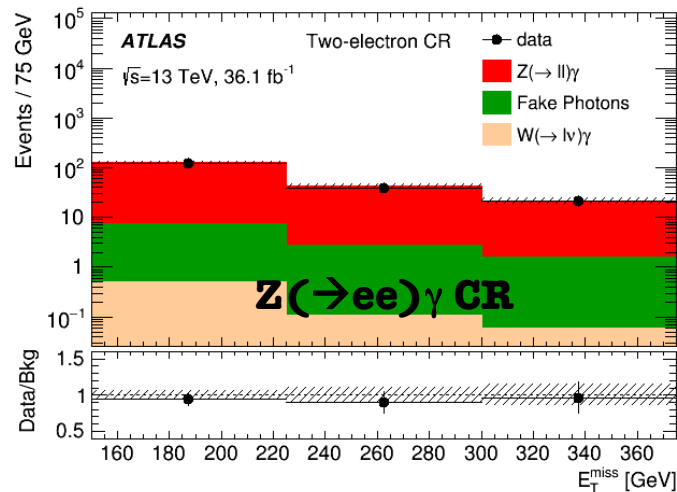
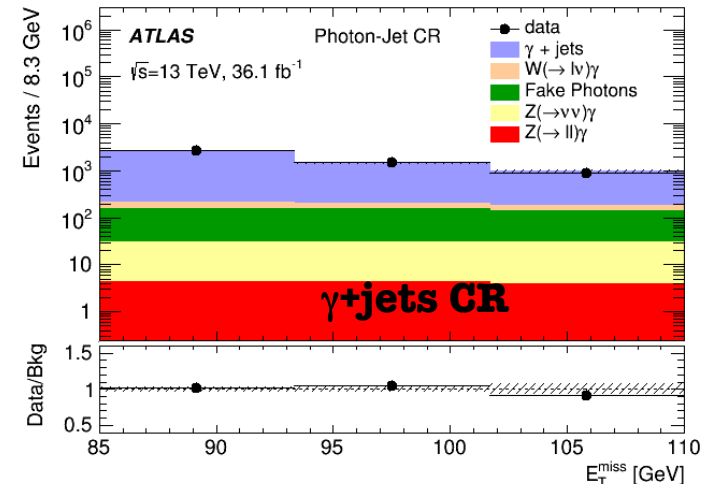
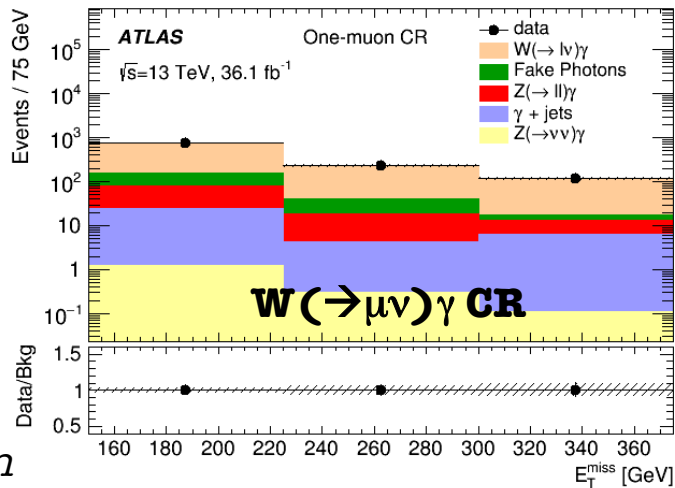
Performance: Jets/ E_T^{miss}



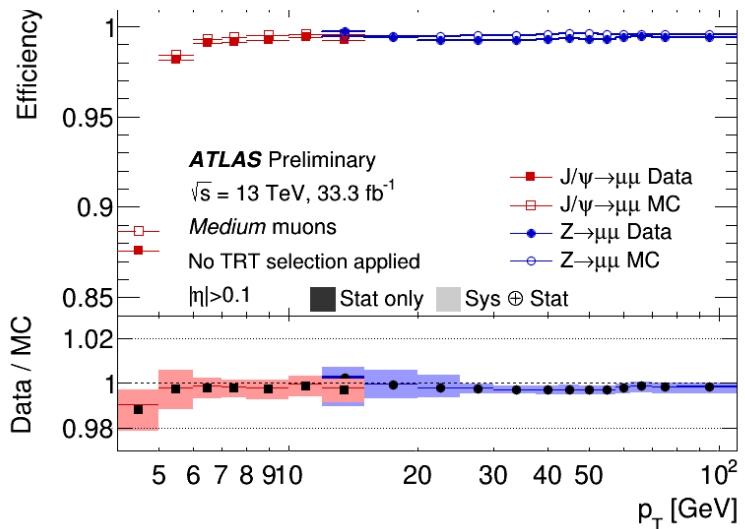
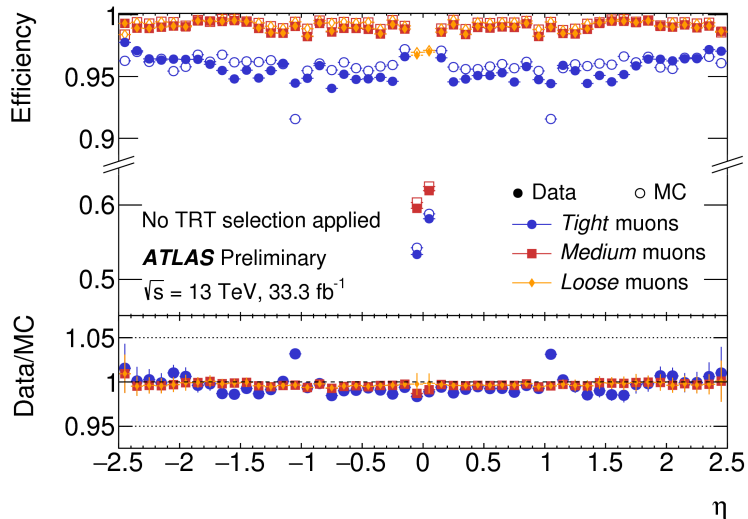
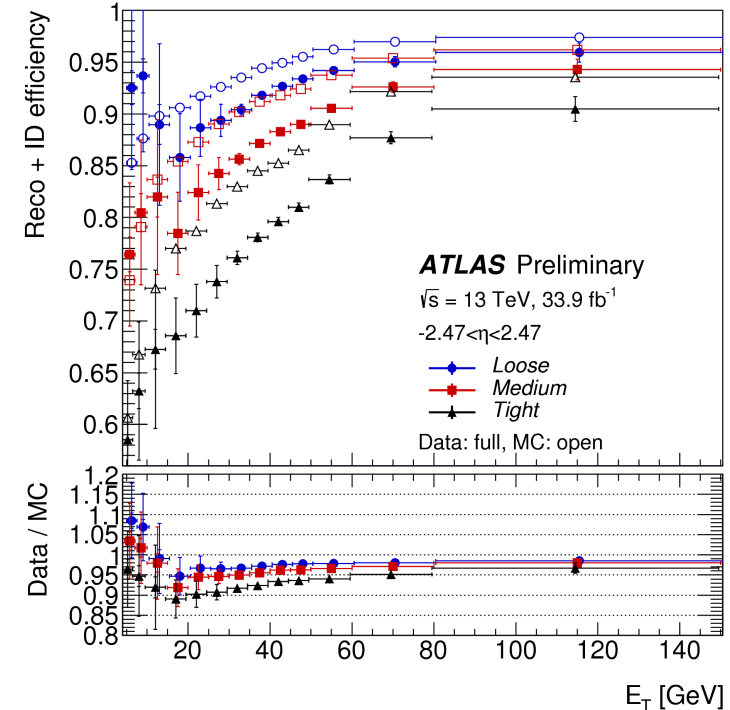
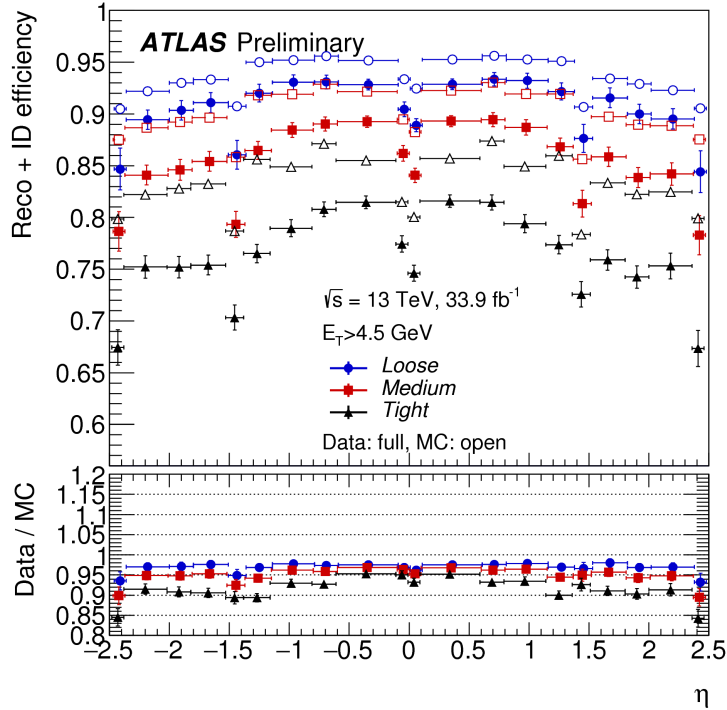
Photon + E_T^{miss} Search

- **High p_T photon.**
 - $p_T > 150 \text{ GeV}$, $|\eta| < 2.37$, tight, isolated.
- **$E_T^{\text{miss}} > 150 \text{ GeV}$.**
 - $\Delta\phi(\gamma, E_T^{\text{miss}}) > 0.4$
- $N_{\text{jets}}(p_T > 30 \text{ GeV}, |\eta| < 4.5) \leq 1$
- $\Delta\phi(E_T^{\text{miss}}, \text{jet}) > 0.4$.
- **SR:** veto on muons ($p_T > 6 \text{ GeV}$) and electrons ($p_T > 7 \text{ GeV}$).

Multiple CRs defined to constrain SM backgrounds (*inverting lepton vetoes, or in different E_T^{miss} regions*).



Performance: Leptons



Dilepton Search

Strategy

- Main background from Drell-Yan production. Additional contributions from processes including 2 real leptons in the final state (t-tbar, single top quark, diboson).
- Estimated using MC samples.

DY events are simulated with NLO Powheg generator.

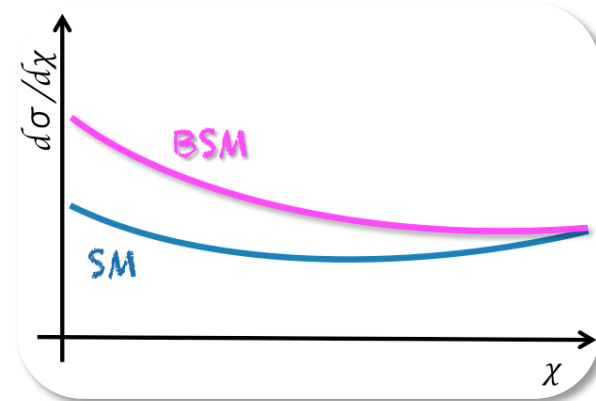
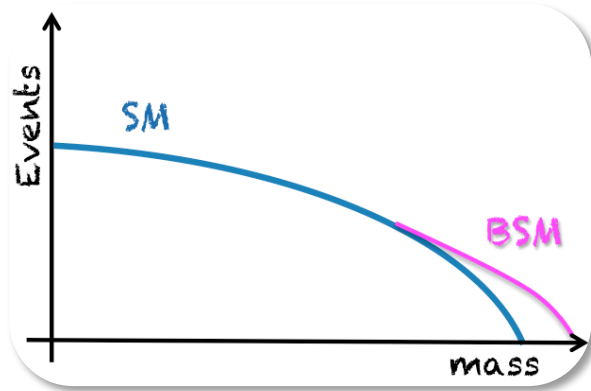
Events yields are corrected with mass dependent rescaling from NLO to NNLO QCD. Mass-dependent EW-corrections at NLO are also applied.

- *Fakes* background: multijet and W+jets events, where one or more jets satisfies the lepton selection.
 - Negligible in di-muon channel.
 - Using data-driven approach: *matrix method*. Measure fake (**f**) and real (**r**) rates: probabilities of a jet or an electron **to be identified as an electron**.

$$\begin{pmatrix} N_{TT} \\ N_{TL} \\ N_{LT} \\ N_{LL} \end{pmatrix} = \begin{pmatrix} r^2 & rf & fr & f^2 \\ r(1-r) & r(1-f) & f(1-r) & f(1-f) \\ (1-r)r & (1-r)f & (1-f)r & (1-f)f \\ (1-r)^2 & (1-r)(1-f) & (1-f)(1-r) & (1-f)^2 \end{pmatrix} \begin{pmatrix} N_{RR} \\ N_{RF} \\ N_{FR} \\ N_{FF} \end{pmatrix} \quad N_{TT}^{\text{Multi-jet \& W+jets}} = rf(N_{RF} + N_{FR}) + f^2 N_{FF}$$

- N_{RF} , N_{FR} , and N_{FF} obtained through matrix inversion
expressed in terms of measurable quantities: N_{TT} , N_{TL} , N_{LT} , N_{LL})

Motivation



CI in **mass** distributions:

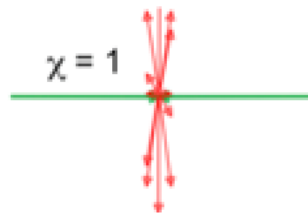
- Observable as broad excess in dilepton invariant mass spectrum.
- Observation in m_{ll} distribution requires precise understanding of QCD cross section.

CI in **angular** distributions:

- CI is often more isotropic than QCD.
 - As function of $\cos\theta^*$.
- Angular distributions have much smaller systematic uncertainties than cross section vs m_{jj} .
- Some sensitivity to resonant signals too.

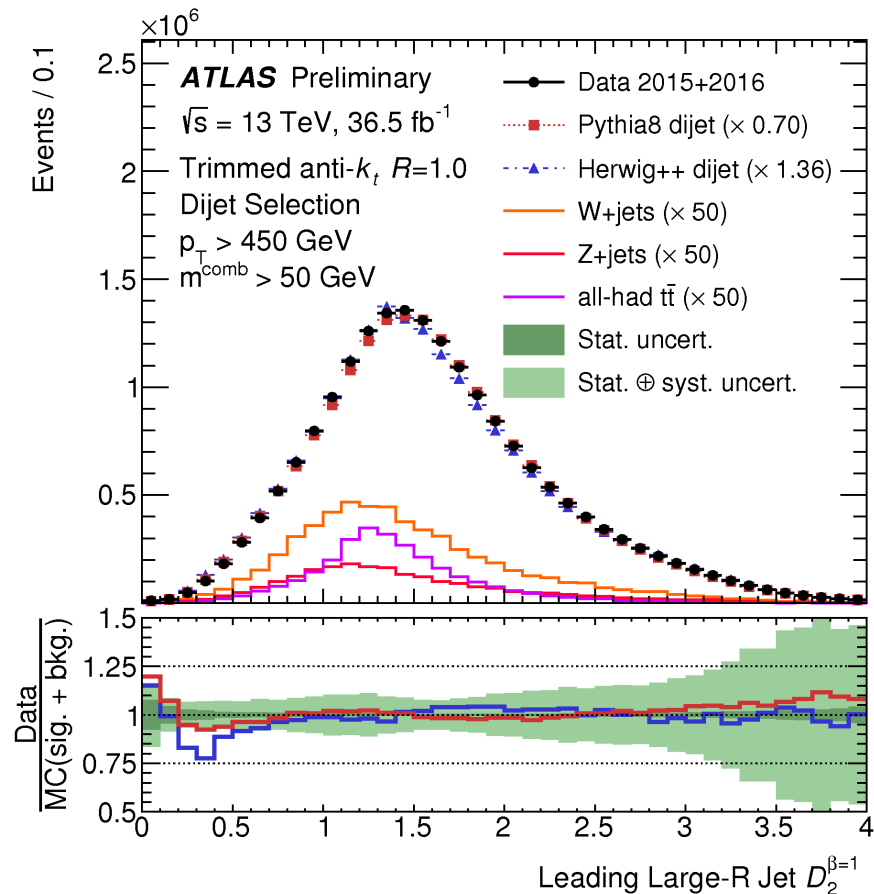
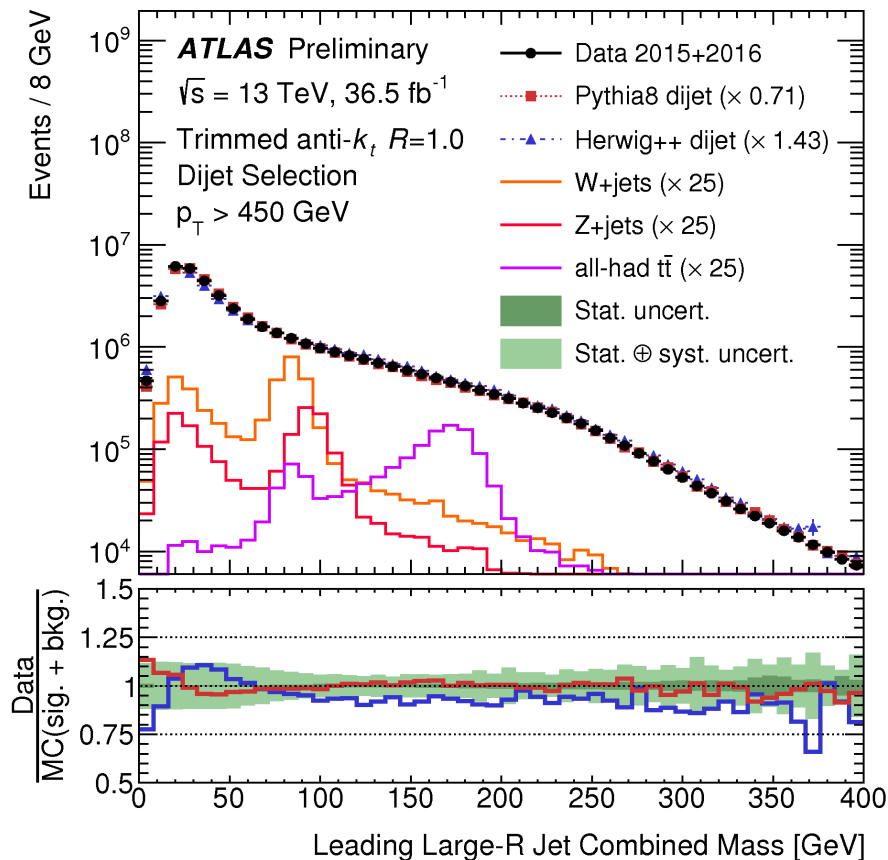
more BSM-like

more QCD-like



$$\chi = e^{2|y^*|} \sim \frac{1 + \cos\theta^*}{1 - \cos\theta^*}$$

Performance: *Boson Tagging*



Standard Model

Phys. Lett. B 716 (2012) 1-29

The **Higgs discovery** further validated the SM
(*self-consistent theory*).

Run I legacy: Higgs discovery
The discovery of a new particle
also opened a new channel for
searches.

Still left with many open
questions....

e.g. High-levels of **fine tuning**
needed to avoid divergences in
Higgs mass corrections.

